A NOVEL APPROACH FOR INDUCIBLE, REVERSIBLE GENE REPLACEMENT AND ITS APPLICATION TO THE STUDY OF DREBRIN/EB3 INTERACTION IN DENDRITIC SPINES

by

Matthew M. Millette

A dissertation submitted in partial fulfillment of
the requirements for the degree of

Doctor of Philosophy

(Neuroscience)

at the

UNIVERSITY OF WISCONSIN-MADISON

2018

Date of final oral examination: 6/19/18

The dissertation is approved by the following members of the Final Oral Committee:

Erik Dent, Associate Professor, Neuroscience
Bill Bement, Professor, Zoology
Tim Gomez, Professor, Neuroscience
Jill Wildonger, Assistant Professor, Biochemistry
Justin Williams, Professor, Biomedical Engineering

My most sincere thanks to -

My parents Mike and Kathy, my sister Megan, and my partner Hayley
for their unflagging support, love and encouragement.

My advisor, Erik, for his insight, example, humor and patience.
The path wasn't always clear, but I'm grateful to have been afforded the freedom
to see where it led. I'm a better scientist for the scrapes and gray hairs.

The members of my committee, Dent lab past and present, and joint lab meeting
for thoughtful critique and input.

Friends near and far who've been there along the way.

TABLE OF CONTENTS

Chapter 1

Introduction

Overview

Changes in the molecular content of dendritic spines precede and are necessary for long-term potentiation (LTP), widely considered a cellular substrate of learning and memory. New receptors, channels, scaffolding proteins, and myriad other components must be delivered and incorporated into individual synapses to strengthen their connections with other neurons. As neurons mature they acquire elaborate, functionally specialized architectures, and as they become more complex so do the logistics of delivering these materials. An unresolved question is how these cargoes are delivered efficiently, but recent work from our lab and others suggests activity-dependent cytoskeletal coordination is instrumental in this. Thus, the first goal of this work has been to understand how the actin cytoskeleton preferentially directs transient entry of microtubules, and cargo transported along them, to individual synapses undergoing plasticity. While this line of research has merit in satisfying basic curiosity regarding the “gears and cogs” which drive our cognition, it is also important from a medical perspective, as the same mechanisms are vulnerable to dysregulation in common but debilitating diseases such as Alzheimer’s. This work has required the development of streamlined, versatile, genetically encoded tools to study the impact of functional mutations in mature neurons. The second overarching goal has been the refinement of this inducible knockdown-rescue (KDR) strategy for replacing endogenous protein of interest with experimental constructs. While originally conceived as a platform as a means of perturbing healthy cells to understand the effects of targeted mutations, in case of diseases with genetic etiology, we envision that with appropriate advances in therapeutic vectors the reverse is also quite possible. Though tools devised for basic research are rarely directly translatable to clinical application, we designed this technique to be easily portable and entirely vector agnostic. Therefore, future advances in viral

therapeutics may be harnessed without undue complication, enhancing, rather than antiquating this strategy.

Microtubule dynamics both support and are influenced by synaptic plasticity

Microtubules (MTs) are hollow, polar polymers composed of α/β-tubulin heterodimers which undergo sporadic bouts of polymerization and depolymerization at their plus ends. These bouts of growth, pausing, and shrinkage termed “dynamic instability” permit MTs to efficiently explore intracellular space (Mitchison & Kirschner 1984). This behavior is governed by a vast array of MT-associated proteins (MAPs) which modify MT stability (Akhmanova & Steinmetz 2015; Bowne-Anderson et al., 2015), bundling (Walczak & Shaw 2010), severing (Roll-Mecak & Mcnally 2010) and nucleation of new MTs (Yu et al., 1993; Sánchez-Huertas et al., 2016). Post-translational modifications provide an additional regulatory layer with an impressive range of functionally intertwined consequences (Gadadhar et al., 2017). For example, tubulin detyrosination inhibits Kif2C and Kif2A motors from disassembling MTs (Peris et al., 2009), but increases the landing rate of Kif5 on MTs (Kaul et al., 2014), while activity-enhanced polyglutamylation increases Kif5-dependent transport velocity of postsynaptic cargos in neurons (Maas et al., 2009).

Studying these complex, interrelated factors and the function of dynamic MTs in living cells has always presented challenges. Prior to the advent and accessibility of genetically encoded fluorescent fusion proteins, pioneering cytoskeletal biologists microinjected and imaged dye-conjugated tubulin into fertilized sea urchin eggs. This permitted early demonstration that MT polymerization is rapid *in vivo*, and that temporally and spatially regulated assembly is required for proper cell division (Wadsworth et al., 1983). Years later, technically demanding experiments employed a similar approach to visualize MT dynamics in

developing cortical neurons. This provided the first direct evidence that reorganization and movement of individual MTs occurs in both growth cones and interstitial branches (Dent et al., 1999). Despite downright athletic participation in the functional establishment of neurons (Dent et al., 2011; Kapitein and Hoogenraad 2015) and data indicating that at least a fraction of MTs remain dynamic in adulthood (Baas et al., 1991; Brown et al., 1993) the historically prevailing notion was that the MT cytoskeleton collectively became a hard-set, static structure as neurons reached maturity. This rigid network would serve to maintain structural and synaptic architecture, and to provide a network of railways for transport from the soma to the periphery, to support fine-scale plasticity between those connections. One could speculate this assumption was bolstered by the technical obstacle the naturally dense array of MTs in the dendritic shaft poses to conventional light microscopy. However, it is becoming clearer that dynamic MTs are indispensable for learning and memory at all neuronal stages.

Several of the first sources of evidence *in vivo* center on stathmin, a phospho-regulated inhibitor of MT assembly (Belmont et al., 1996; Redeker et al., 2000). For example, acute amygdalar slices from stathmin knockout mice exhibit deficits in long-term potentiation (LTP), and behavioral assessments reveal these animals are impaired in both innate and learned fear responses. Further, LTP in this same cortico-amygdala pathway is vulnerable to taxol, a MT stabilizing drug (Shumyatsky et al., 2005). Contextual fear conditioning, a predominantly hippocampal form of memory, is also vulnerable to MT manipulation as treatment of animals with nocodazole, a MT-depolymerizing drug, impairs fear acquisition and reduces dendritic spine density (Fanara et al., 2010). Interestingly, co-administration of nocodazole and taxol, to effect no net change in dynamics, causes no such deficits (Uchida et al., 2014). While these demonstrations that genetic and pharmacological interference with MT dynamics impairs learning were informative, the bigger revelation from these publications was that MT turnover

naturally accompanies learning, and might even be considered a biomarker of synaptic plasticity. Fanara et al., showed that fear conditioning increased the turnover of stable, MAP2-associated and cold stable MTs in the hippocampus. In alignment with this study, Uchida et al., later showed that MT stability is regulated in a biphasic manner by learning. During early LTP, activity-dependent stathmin phosphorylation results in its detachment from tubulin and a concomitant temporary increase in MT dynamics, whereas at baseline, stathmin is unphosphorylated and MTs are more stable. Yet, precisely how these changes contribute to learning and memory is still being unraveled.

Cytoskeletal elements vary in their organization and composition based on their subcellular location in neurons. For example, it is long-established that axonal MTs are uniformly oriented plus end distal, while dendritic MTs are of mixed polarity (Baas et al., 1988). Dendrites are further characterized by compartmentalization of actin in dendritic spines, which serves as a structural element to support spine structure and organize postsynaptic machinery (Hlushchenko et al., al 2016). Despite incidental documentation to the contrary over the span of decades (Westrum et al., 1980, Gray et al., 1982, Chicurel et al., 1992, Fiala et al., 2003, Mitsuyama et al., 2008), the notion that MTs are strictly confined to the dendritic shaft has only been decidedly overturned in recent years. Initial observations of MTs in spines were broadly dismissed as artifacts of unconventional dissection media, cooling and warming of tissue during the EM fixation process, or otherwise waved off as trivial oddities. However, through dedicated, purposeful live imaging of GFP-tubulin expressed in mature cultured neurons our lab found that MTs, in fact, frequently enter dendritic spines. These “invasions,” as they will be referred to for the remainder of this dissertation, are transient, lasting seconds to minutes, and previous characterization suggests that at baseline about 1% of spines contain a MT at any given moment, with roughly 10% of spines targeted per hour (Hu et al., 2008). This phenomenon has

since been observed in a variety of cell types including cortical (Hu et al., 2008), hippocampal (Gu et al., 2008; Hu et al., 2008; Jaworski et al., 2009; Merriam et al., 2013) and Purkinje neurons (Wagner et al., 2011).

Changes in the structure, organization, and molecular composition of dendritic spines are required for LTP, and critical for learning and memory (Xu et al., 2009; Yang et al., 2009; Hübener and Bonhoeffer, 2010). Many components of the postsynaptic density (PSD) are shuttled along MTs from the soma and into the dendrites by kinesin motor proteins (Verhey et al., 2011) and cytoplasmic dynein (Cianfrocco et al., 2015). Prior to the observation of transient MT polymerization events into dendritic spines there were two predominant models of how this cargo was transferred from the dendritic shaft and incorporated into the PSD of the dendritic spine. The first model proposes that, at some point along this journey, cargo is released directly beneath a dendritic spine and reaches the PSD through diffusion (Guillaud et al., 2008). Similarly, receptors incorporated into the membrane of the dendrite itself can drift laterally into spines and make their way to the PSD . Secondly, a “hand-off” model has been proposed where control of cargo carried along MTs by kinesin and dynein motors must be transferred to actin-based myosin motors, which may be resident in spines or already attached to the cargo vesicle itself (Ryan et al., 2005; Desnos et al., 2007; Correia et al., 2008). Even with the possibility that diffusive signaling molecules in the spine neck and base locally release cargo from MTs (McVicker et al., 2015), both of these models are deficient in terms of specificity if the task is to selectively bolster synapses undergoing LTP with critical materials, rather than potentially quiescent neighbors. Excitingly, our lab recently showed that the MT-based motor protein KIF1A transports synaptotagmin (syt) family member syt4 directly into spines. Further, with ph-sensitive superecliptic phluorin (SEP) constructs, which fluoresce when exocytosed into the membrane, we also showed functional synaptic incorporation (McVicker et al., 2016). After

years of speculation this conclusively demonstrated that a direct-deposit scheme, facilitated by transient MT invasion of spines, supplies postsynaptic cargo into specific dendritic spines. Moreover, once within a spine MTs can frequently be observed tracking multiple short growth and shrinkage events before disappearing from view entirely, indicating that MT was stable for the remainder of the time-lapse or depolymerized completely back down to the dendritic shaft. Importantly, while MT polymerization rates average roughly 0.2-0.3μm/sec (Gierke et al., 2010), kinesins travel along MTs at 0.5-2μm/sec, which is rapid enough to visually track their plus ends (Wu et al., 2006). Thus, even in the absence of further signaling, stochastic MT catastrophe while within spines should provide an adequate means to release motors and postsynaptic cargo directly within the head of the spine.

However, MT-based “direct-deposit” provides little practical advantage over other transport modalities unless MTs preferentially target synaptically active spines. Crucially, initial characterizations of MT-spine invasion events illustrate precisely this. Stimulating global neuronal activity with short pulses of KCl increases invasion occurrence three-fold over baseline, and inhibition by global voltage-gated sodium channel blockade with tetrodotoxin (TTX) dramatically reduces this rate (Hu et al., 2008). Similarly, chelation of extracellular calcium by BAPTA-AM dramatically reduces the number of MTs entering spines (Merriam et al., 2013). Induction of a chemical LTP (cLTP) protocol by NMDA receptor unmasking with Gly-0Mg^{++} also increases both the number of spines targeted and frequency of events (Merriam et al., 2011). In line with this, induction of long-term depression (LTD) following NMDA receptor hyper-activation decreases MT invasions (Kapitein et al., 2011). Further, by monitoring calcium dynamics with the genetically encoded indicator GCaMP our lab has shown that transient calcium spikes are predictive of invasion at the single-spine level (Merriam et al., 2013). Interestingly, spines that are invaded by MTs after activation of NMDA receptors show a marked

increase in size as opposed to spines that are not invaded, while pre-treatment with nanomolar concentrations of nocodazole, which inhibits MT dynamics and prevents MT invasion of spines, completely eliminates this NMDA-mediated increase in spine size (Merriam et al., 2011). Given that spine volume and morphology are established positive correlates of function (Matsuzaki et al., 2004), these studies demonstrate that initial stages of plasticity itself inform which spines are to be targeted. Further, that some function, or some collection of functions, of MT entry into spines is necessary for plasticity.

Actin-based synaptic tagging guides microtubules into specific dendritic spines

Signaling events downstream of synaptic calcium influx result in rapid and major rearrangement of the actin cytoskeleton within individual spines (Cingolani and Goda, 2008; Kasai et al., 2010). Expression of LTP *in vitro* requires subsequent filamentous actin (F-actin) polymerization (Krucker et al., 2000; Matsuzaki et al., 2004; Honkura et al., 2008), and preventing actin assembly *in vivo* interferes with learning and memory (Fukazawa et al., 2003; Fischer et al., 2004; Ramachandran and Frey 2009). Indeed, actin polymerization itself has been proposed as a candidate “synaptic tag” (Okamoto et al., 2009; Ramachandran and Frey 2009; Rogerson et al., 2014), which, by definition, is a means to transiently mark a synapse after activation such that it is recognized as requiring new components to effect an enduring change in transmission efficiency. In line with this, we have previously demonstrated that increases of F-actin content within individual spines are predictive of MT entry. Moreover, F-actin polymerization is both necessary and sufficient for MT invasions because pharmacologically polymerizing F-actin increases the rate of MT entry, while depolymerizing F-actin all but eliminates these events (Merriam et al., 2013). Though F-actin is by-and-large restricted to spines in dendrites, it transiently polymerizes out the spine neck and base where it

is ideally positioned to interact with MTs (Honkura et al., 2008; Korobova & Svitkina 2010). However, actin and tubulin have no direct affinity to one another, so any coordinated action of the two cytoskeletons is regulated by intermediate binding partners.

We are particularly interested in evaluating MT plus end tracking proteins (+TIPs) as interfaces between actin and MTs to guide invasions. Perez et al. (1999) first demonstrated that a chimeric CLIP-170-GFP fusion selectively and transiently aggregated onto actively polymerizing, GTP-bound tubulin. Discovery of additional +TIPs followed in short order, including CLIP-170, XMAP215, and EB family proteins which, despite diverse tubulin binding interfaces, share the common property of promoting tubulin assembly as polymerization chaperones (Slep and Vale 2007). EB family proteins in particular act as the base-layer of important functional complexes (Lansbergen and Akhmanova 2006; Kumar and Wittmann 2012). In fact, by number, most proteins that localize to polymerizing MT plus ends do so by virtue of EB affinity (Stepanova et al., 2003; Akhmanova & Steinmetz 2010). In the central nervous system (CNS), there are two EB family isoforms: EB1 which is ubiquitous, and EB3, which is preferentially expressed in nervous tissue (Nakagawa et al., 2000). In cultured hippocampal neurons the EB1:EB3 ratio increases dramatically after 10 DIV (Jaworski et al., 2009). While EB1 and EB3 only share 54% sequence identity, their functional domains are largely conserved. Both have an N-terminal calponin homology domain which binds tubulin, and while it remains unclear whether EBs are obligate dimers (Slep and Vale 2007; *contrast with* Komarova et al., 2009; Skube 2010), the C-terminal EB homology domain is responsible for homodimerization and heterodimerization (Akhmanova and Steinmetz, 2010). The C-terminus of EB family proteins also features two established modes of anchoring plus end complexes. First, a further functional subdivision of the the EB-homology domain recognizes SxIP (serine-any amino acid-isoleucine-proline) motifs in EB-associated proteins. This domain is

commonly referred to as the Adenomatous Polyposis Coli protein (APC)-binding domain, as APC was the first discovered EB1 binding partner (Su et al., 1995). These SxIP recognition motifs act as +TIP localization signals and, preferentially, reside within basic proline- and serine-rich regions, whose sequences are not otherwise conserved (Kumar and Wittmann 2012). Secondarily, a cytoskeleton-associated protein-glycine-rich (CAP-Gly) domain is located at the utmost residues of both EB1 and EB3 and relies on their terminal tyrosine. This is a feature shared with tubulin itself, which interacts with zinc-finger motifs and proline-rich sequences (Steinmetz and Akhmanova 2008). As should be expected from the aforementioned studies, genetic depletion of EB3 has significant effects on dendritic spines. In cultured neurons EB3 silencing reduces total spine density (Gu et al., 2008) and reverts spines to a morphologically immature appearance (Jaworski et al., 2009). Considering the aforementioned functions of EB family proteins, the sweeping nature of these manipulations answers few questions. It should be noted that it remains undocumented whether EB3 silencing reduces MT invasions of spines. Thus, further focused study is necessary to determine the importance of specific intermediates in directing spine invasions.

One promising actin-associated candidate is drebrin (developmentally regulated brain protein). In neurons drebrin is found in two major isoforms which arise from splice variation. One “embryonic” (E) isoform, which is expressed in many types of cells and tissues, and one “adult” (A) isoform, whose expression is exclusively neuronal and increases as cells develop (Kojima et al.,1993; Peitsch et al., 1999; Keon et al., 2000; Jin et al. et al., 2002; Aoki et al. et al., 2005). Drebrin E and A are identical, save for 46 amino acids (residues 321-365) present in drebrin A. Mutant mice which never produce the drebrin A isoform exhibit deficits in both conditioned fear response and hippocampal LTP (Kojima et al, et al., 2010; Kojima et al., 2016), though the exact mechanisms behind this phenotype remain unclear. Nevertheless, developmental studies

report that drebrin-EB3 interaction is involved in neuritogenesis (Geraldo et al., 2008), and axon collateral branching (Ketschek et al., 2016). This association appears specific to the EB3 isoform (Geraldo et al., 2008), and enhanced by drebrin S142 phosphorylation (Worth et al., 2013). In our hands, drebrin A overexpression potently upregulates MT invasions of spines in mature hippocampal cultures (Merriam et al., 2013). Additionally, deletion of EB3 residues 177-194 appears to eliminate its association with drebrin, however this region is recognized by no other known binding partners, and represents an unconventional mode of interaction (Geraldo et al., 2008). To date, no motif or domain has been identified within drebrin that directly interacts with EB3. Taking these data into consideration, a major focus of my graduate work has been evaluating the contributions of EB3 and drebrin as putative MT-actin cross-linkers in the guidance of MTs into spines, and is detailed in Chapter 2 of this dissertation.

Advantages and Challenges of Primary Neuron Culture in the Study of Invasions

Rodent hippocampal neurons are a favored model to study the cellular and molecular bases of learning and memory. Despite wishes to minimize animal usage and the conveniences inherent to immortalized cell lines, to date there has been no satisfactory demonstration that neurons differentiated from IPSCs or ESCs approach the quality or reliability of cultured primary hippocampal neurons. All alternatives considered, until major advances are made in this realm it is not possible to conduct these experiments outside of primary cells. MT dynamics are difficult to study under the best circumstances, but this becomes a task of still greater magnitude when dissecting the contributions of specific functional elements that govern their behavior in mature neurons. Dominant-negative experiments are routine in such ventures. For example, overexpressing an isolated functional domain of a protein will saturate a system and compete

for binding sites of endogenous protein. How a dominant negative perturbs a system can be highly informative, but is prone to mis- and over-interpretation.

More as a rule than as an exception, proteins of interest will serve multiple roles within complex biological systems. Drebrin illustrates this point well. In addition to its critical modulation of the actin cytoskeleton (Ishikawa et al., 1994; Sasaki et al., 1996; Grintsevich et al., 2014) drebrin has myriad other functions via diverse binding partners. In neurons, it has been implicated in the generation of new dendritic spines (Yamazaki et al., 2014), in the trafficking of critical postsynaptic components such as NMDA receptor subunits (Aoki et al., 2009; Chen at al., 2017) and PSD-95 (Mizui et al., 2005), and in the functional organization of those components in complexes during maturity (Shiraishi-Yamaguchi et al., 2009). This issue is compounded when proteins of interest serve roles across the extensive and intricate development of neurons, where practically any functional mutation worth examining in synaptic plasticity should be expected to impact development in some manner. If we are to understand how proteins of interest function in maturity, manipulations should be timed appropriately to preserve earlier stages. Additionally, when these functions are complementary it becomes worrisome that a net-positive effect of endogenous “background” expression, or even modest mutant overexpression will obscure an otherwise critical function eliminated by a targeted, specific mutation. Direct gene editing, as with CRISPR/Cas9, is an attractive approach to avoid these issues in many systems, but is not practical in primary neurons on account of poor efficiency and extensive validation required to ensure even simple mutations have been introduced correctly.

If we are to understand how proteins of interest function in neuronal maturity, manipulations should be timed appropriately to preserve earlier stages of development. Moreover, if our goal is to determine how important one specific functional mutation is toward

promoting MT invasions of spines, then it is imperative that mutants constructs be studied in the absence of background endogenous expression, and that our “rescue” gene be expressed at physiologically relevant levels. At present, the concept of a knock-down replacement strategy to study protein function has not been implemented in any methodical way, and tools presently available to carry out the experiments described here are heavily limited in their application to neuroscience. To address these issues we developed a novel system to carry out complete, physiologically-matched genetic replacement of proteins of interest using an inducible, modular plasmid. In Chapter 3 of this dissertation we describe the conception and development of these materials and demonstrate its use as a means to effectively deliver optogenetic probes. In Chapter 2, we apply this strategy to probe putative drebrin-EB3 interacting regions as they pertain to the guidance of MTs into dendritic spines. Finally, in Chapter 4 we summarize our findings and propose future directions of this research.

References

Akhmanova A, Steinmetz MO. Control of microtubule organization and dynamics: two ends in the limelight. Nat Rev Mol Cell Biol. 2015;16(12):711-26.

Akhmanova A, Steinmetz MO. Microtubule +TIPs at a glance. J Cell Sci. 2010;123(Pt 20):3415-9.

Aoki C, Kojima N, Sabaliauskas N, et al. Drebrin a knockout eliminates the rapid form of homeostatic synaptic plasticity at excitatory synapses of intact adult cerebral cortex. J Comp Neurol. 2009;517(1):105-21.

Aoki C, Sekino Y, Hanamura K, et al. Drebrin A is a postsynaptic protein that localizes in vivo to the submembranous surface of dendritic sites forming excitatory synapses. J Comp Neurol. 2005;483(4):383-402.

Baas PW, Deitch JS, Black MM, Banker GA. Polarity orientation of microtubules in hippocampal neurons: uniformity in the axon and nonuniformity in the dendrite. Proc Natl Acad Sci USA. 1988;85(21):8335-9.

Baas PW, Slaughter T, Brown A, Black MM. Microtubule dynamics in axons and dendrites. J Neurosci Res. 1991;30(1):134-53.

Belmont LD, Mitchison TJ. Identification of a protein that interacts with tubulin dimers and increases the catastrophe rate of microtubules. Cell. 1996;84(4):623-31.

Bowne-Anderson H, Hibbel A, Howard J. Regulation of Microtubule Growth and Catastrophe: Unifying Theory and Experiment. Trends Cell Biol. 2015;25(12):769-79.

Brown A, Li Y, Slaughter T, Black MM. Composite microtubules of the axon: quantitative analysis of tyrosinated and acetylated tubulin along individual axonal microtubules. J Cell Sci. 1993;104 (Pt 2):339-52.

Chicurel ME, Harris KM. Three-dimensional analysis of the structure and composition of CA3 branched dendritic spines and their synaptic relationships with mossy fiber boutons in the rat hippocampus. J Comp Neurol. 1992;325(2):169-82.

Cianfrocco MA, Desantis ME, Leschziner AE, Reck-peterson SL. Mechanism and regulation of cytoplasmic dynein. Annu Rev Cell Dev Biol. 2015;31:83-108.

Cingolani LA, Goda Y. Actin in action: the interplay between the actin cytoskeleton and synaptic efficacy. Nat Rev Neurosci. 2008;9(5):344-56.

Correia SS, Bassani S, Brown TC, et al. Motor protein-dependent transport of AMPA receptors into spines during long-term potentiation. Nat Neurosci. 2008;11(4):457-66.

Dent EW, Callaway JL, Szebenyi G, Baas PW, Kalil K. Reorganization and movement of microtubules in axonal growth cones and developing interstitial branches. J Neurosci. 1999;19(20):8894-908.

Dent EW, Gupton SL, Gertler FB. The growth cone cytoskeleton in axon outgrowth and guidance. Cold Spring Harb Perspect Biol. 2011;3(3)

Desnos C, Huet S, Darchen F. 'Should I stay or should I go?': myosin V function in organelle trafficking. Biol Cell. 2007;99(8):411-23.

Fanara P, Husted KH, Selle K, et al. Changes in microtubule turnover accompany synaptic plasticity and memory formation in response to contextual fear conditioning in mice. Neuroscience. 2010;168(1):167-78.

Fiala JC, Kirov SA, Feinberg MD, et al. Timing of neuronal and glial ultrastructure disruption during brain slice preparation and recovery in vitro. J Comp Neurol. 2003;465(1):90-103.

Fischer A, Sananbenesi F, Schrick C, Spiess J, Radulovic J. Distinct roles of hippocampal de novo protein synthesis and actin rearrangement in extinction of contextual fear. J Neurosci. 2004;24(8):1962-6.

Fukazawa Y, Saitoh Y, Ozawa F, Ohta Y, Mizuno K, Inokuchi K. Hippocampal LTP is accompanied by enhanced F-actin content within the dendritic spine that is essential for late LTP maintenance in vivo. Neuron. 2003;38(3):447-60.

Gadadhar S, Bodakuntla S, Natarajan K, Janke C. The tubulin code at a glance. J Cell Sci. 2017;130(8):1347-1353.

Geraldo S, Khanzada UK, Parsons M, Chilton JK, Gordon-weeks PR. Targeting of the F-actin-binding protein drebrin by the microtubule plus-tip protein EB3 is required for neuritogenesis. Nat Cell Biol. 2008;10(10):1181-9.

Gierke S, Kumar P, Wittmann T. Analysis of microtubule polymerization dynamics in live cells. Methods Cell Biol. 2010;97:15-33.

Gray EG, Westrum LE, Burgoyne RD, Barron J. Synaptic organisation and neuron microtubule distribution. Cell Tissue Res. 1982;226(3):579-88.

Grintsevich EE, Reisler E. Drebrin inhibits cofilin-induced severing of F-actin. Cytoskeleton (Hoboken). 2014;71(8):472-83.

Gu J, Firestein BL, Zheng JQ. Microtubules in dendritic spine development. J Neurosci. 2008;28(46):12120-4.

Guillaud L, Wong R, Hirokawa N. Disruption of KIF17-Mint1 interaction by CaMKII-dependent phosphorylation: a molecular model of kinesin-cargo release. Nat Cell Biol. 2008;10(1):19-29.

Hlushchenko I, Koskinen M, Hotulainen P. Dendritic spine actin dynamics in neuronal maturation and synaptic plasticity. Cytoskeleton (Hoboken). 2016;73(9):435-41.

Honkura N, Matsuzaki M, Noguchi J, Ellis-davies GC, Kasai H. The subspine organization of actin fibers regulates the structure and plasticity of dendritic spines. Neuron. 2008;57(5):719-29.

Hu X, Viesselmann C, Nam S, Merriam E, Dent EW. Activity-dependent dynamic microtubule invasion of dendritic spines. J Neurosci. 2008;28(49):13094-105.

Hübener M, Bonhoeffer T. Searching for engrams. Neuron. 2010;67(3):363-71.

Ishikawa R, Hayashi K, Shirao T, et al. Drebrin, a development-associated brain protein from rat embryo, causes the dissociation of tropomyosin from actin filaments. J Biol Chem. 1994;269(47):29928-33.

Jaworski J, Kapitein LC, Gouveia SM, et al. Dynamic microtubules regulate dendritic spine morphology and synaptic plasticity. Neuron. 2009;61(1):85-100.

Jin M, Tanaka S, Sekino Y, et al. A novel, brain-specific mouse drebrin: cDNA cloning, chromosomal mapping, genomic structure, expression, and functional characterization. Genomics. 2002;79(5):686-92.

Kapitein LC, Hoogenraad CC. Building the Neuronal Microtubule Cytoskeleton. Neuron. 2015;87(3):492-506.

Kapitein LC, Yau KW, Gouveia SM, et al. NMDA receptor activation suppresses microtubule growth and spine entry. J Neurosci. 2011;31(22):8194-209.

Kasai H, Fukuda M, Watanabe S, Hayashi-takagi A, Noguchi J. Structural dynamics of dendritic spines in memory and cognition. Trends Neurosci. 2010;33(3):121-9.

Kaul N, Soppina V, Verhey KJ. Effects of α-tubulin K40 acetylation and detyrosination on kinesin-1 motility in a purified system. Biophys J. 2014;106(12):2636-43.

Keon BH, Jedrzejewski PT, Paul DL, Goodenough DA. Isoform specific expression of the neuronal F-actin binding protein, drebrin, in specialized cells of stomach and kidney epithelia. J Cell Sci. 2000;113 Pt 2:325-36.

Ketschek A, Spillane M, Dun XP, Hardy H, Chilton J, Gallo G. Drebrin coordinates the actin and microtubule cytoskeleton during the initiation of axon collateral branches. Dev Neurobiol. 2016;76(10):1092-110.

Kojima N, Hanamura K, Yamazaki H, Ikeda T, Itohara S, Shirao T. Genetic disruption of the alternative splicing of drebrin gene impairs context-dependent fear learning in adulthood. Neuroscience. 2010;165(1):138-50.

Kojima N, Shirao T, Obata K. Molecular cloning of a developmentally regulated brain protein, chicken drebrin A and its expression by alternative splicing of the drebrin gene. Brain Res Mol Brain Res. 1993;19(1-2):101-14.

Kojima N, Yasuda H, Hanamura K, Ishizuka Y, Sekino Y, Shirao T. Drebrin A regulates hippocampal LTP and hippocampus-dependent fear learning in adult mice. Neuroscience. 2016;324:218-26.

Komarova Y, De groot CO, Grigoriev I, et al. Mammalian end binding proteins control persistent microtubule growth. J Cell Biol. 2009;184(5):691-706.

Korobova F, Svitkina T. Molecular architecture of synaptic actin cytoskeleton in hippocampal neurons reveals a mechanism of dendritic spine morphogenesis. Mol Biol Cell. 2010;21(1):165-76.

Krucker T, Siggins GR, Halpain S. Dynamic actin filaments are required for stable long-term potentiation (LTP) in area CA1 of the hippocampus. Proc Natl Acad Sci USA. 2000;97(12):6856-61.

Kumar P, Wittmann T. +TIPs: SxIPping along microtubule ends. Trends Cell Biol. 2012;22(8):418-28.

Lansbergen G, Akhmanova A. Microtubule plus end: a hub of cellular activities. Traffic. 2006;7(5):499-507.

Maas C, Belgardt D, Lee HK, et al. Synaptic activation modifies microtubules underlying transport of postsynaptic cargo. Proc Natl Acad Sci USA. 2009;106(21):8731-6.

Matsuzaki M, Honkura N, Ellis-davies GC, Kasai H. Structural basis of long-term potentiation in single dendritic spines. Nature. 2004;429(6993):761-6.

Mcvicker DP, Awe AM, Richters KE, et al. Transport of a kinesin-cargo pair along microtubules into dendritic spines undergoing synaptic plasticity. Nat Commun. 2016;7:12741.

Merriam EB, Millette M, Lumbard DC, et al. Synaptic regulation of microtubule dynamics in dendritic spines by calcium, F-actin, and drebrin. J Neurosci. 2013;33(42):16471-82.

Mitchison T, Kirschner M. Dynamic instability of microtubule growth. Nature. 1984;312(5991):237-42.

Mitsuyama F, Niimi G, Kato K, et al. Redistribution of microtubules in dendrites of hippocampal CA1 neurons after tetanic stimulation during long-term potentiation. Ital J Anat Embryol. 2008;113(1):17-27.

Nakagawa H, Koyama K, Murata Y, Morito M, Akiyama T, Nakamura Y. EB3, a novel member of the EB1 family preferentially expressed in the central nervous system, binds to a CNS-specific APC homologue. Oncogene. 2000;19(2):210-6.

Okamoto K, Bosch M, Hayashi Y. The roles of CaMKII and F-actin in the structural plasticity of dendritic spines: a potential molecular identity of a synaptic tag?. Physiology (Bethesda). 2009;24:357-66.

Peitsch WK, Grund C, Kuhn C, et al. Drebrin is a widespread actin-associating protein enriched at junctional plaques, defining a specific microfilament anchorage system in polar epithelial cells. Eur J Cell Biol. 1999;78(11):767-78.

Perez F, Diamantopoulos GS, Stalder R, Kreis TE. CLIP-170 highlights growing microtubule ends in vivo. Cell. 1999;96(4):517-27.

Peris L, Wagenbach M, Lafanechère L, et al. Motor-dependent microtubule disassembly driven by tubulin tyrosination. J Cell Biol. 2009;185(7):1159-66.

Ramachandran B, Frey JU. Interfering with the actin network and its effect on long-term potentiation and synaptic tagging in hippocampal CA1 neurons in slices in vitro. J Neurosci. 2009;29(39):12167-73.

Redeker V, Lachkar S, Siavoshian S, et al. Probing the native structure of stathmin and its interaction domains with tubulin. Combined use of limited proteolysis, size exclusion chromatography, and mass spectrometry. J Biol Chem. 2000;275(10):6841-9.

Rogerson T, Cai DJ, Frank A, et al. Synaptic tagging during memory allocation. Nat Rev Neurosci. 2014;15(3):157-69.

Roll-Mecak A, Mcnally FJ. Microtubule-severing enzymes. Curr Opin Cell Biol. 2010;22(1):96-103.

Ryan XP, Alldritt J, Svenningsson P, et al. The Rho-specific GEF Lfc interacts with neurabin and spinophilin to regulate dendritic spine morphology. Neuron. 2005;47(1):85-100.

Sánchez-Huertas C, Freixo F, Viais R, Lacasa C, Soriano E, Lüders J. Non-centrosomal nucleation mediated by augmin organizes microtubules in post-mitotic neurons and controls axonal microtubule polarity. Nat Commun. 2016;7:12187.

Sasaki Y, Hayashi K, Shirao T, Ishikawa R, Kohama K. Inhibition by drebrin of the actin-bundling activity of brain fascin, a protein localized in filopodia of growth cones. J Neurochem. 1996;66(3):980-8.

Shiraishi-Yamaguchi Y, Sato Y, Sakai R, et al. Interaction of Cupidin/Homer2 with two actin cytoskeletal regulators, Cdc42 small GTPase and Drebrin, in dendritic spines. BMC Neurosci. 2009;10:25.

Shumyatsky GP, Malleret G, Shin RM, et al. stathmin, a gene enriched in the amygdala, controls both learned and innate fear. Cell. 2005;123(4):697-709.

Skube SB, Chaverri JM, Goodson HV. Effect of GFP tags on the localization of EB1 and EB1 fragments in vivo. Cytoskeleton (Hoboken). 2010;67(1):1-12.

Slep KC, Vale RD. Structural basis of microtubule plus end tracking by XMAP215, CLIP-170, and EB1. Mol Cell. 2007;27(6):976-91.

Steinmetz MO, Akhmanova A. Capturing protein tails by CAP-Gly domains. Trends Biochem Sci. 2008;33(11):535-45.

Stepanova T, Slemmer J, Hoogenraad CC, et al. Visualization of microtubule growth in cultured neurons via the use of EB3-GFP (end-binding protein 3-green fluorescent protein). J Neurosci. 2003;23(7):2655-64.

Su LK, Burrell M, Hill DE, et al. APC binds to the novel protein EB1. Cancer Res. 1995;55(14):2972-7.

Uchida S, Martel G, Pavlowsky A, et al. Learning-induced and stathmin-dependent changes in microtubule stability are critical for memory and disrupted in ageing. Nat Commun. 2014;5:4389.

Wadsworth P, Sloboda RD. Microinjection of fluorescent tubulin into dividing sea urchin cells. J Cell Biol. 1983;97(4):1249-54.

Wagner W, Brenowitz SD, Hammer JA. Myosin-Va transports the endoplasmic reticulum into the dendritic spines of Purkinje neurons. Nat Cell Biol. 2011;13(1):40-8.

Walczak CE, Shaw SL. A MAP for bundling microtubules. Cell. 2010;142(3):364-7.

Westrum LE, Jones DH, Gray EG, Barron J. Microtubules, dendritic spines and spine appratuses. Cell Tissue Res. 1980;208(2):171-81.

Worth DC, Daly CN, Geraldo S, Oozeer F, Gordon-weeks PR. Drebrin contains a cryptic F-actin-bundling activity regulated by Cdk5 phosphorylation. J Cell Biol. 2013;202(5):793-806.

Wu X, Xiang X, Hammer JA. Motor proteins at the microtubule plus-end. Trends Cell Biol. 2006;16(3):135-43.

Xu T, Yu X, Perlik AJ, et al. Rapid formation and selective stabilization of synapses for enduring motor memories. Nature. 2009;462(7275):915-9.

Yamazaki H, Kojima N, Kato K, et al. Spikar, a novel drebrin-binding protein, regulates the formation and stabilization of dendritic spines. J Neurochem. 2014;128(4):507-22.

Yang G, Pan F, Gan WB. Stably maintained dendritic spines are associated with lifelong memories. Nature. 2009;462(7275):920-4.

Yu W, Centonze VE, Ahmad FJ, Baas PW. Microtubule nucleation and release from the neuronal centrosome. J Cell Biol. 1993;122(2):349-59.

Chapter 2

Evaluating EB3-Drebrin Interaction in Microtubule Invasion of Dendritic Spines

Millette MM, Richters KE, Vogel KR, Dent EW. To be submitted.

Author contributions: M.M.M. and E.W.D. conceived the project. M.M.M. performed all cloning, imaging and data analysis. M.M.M. and K.E.R. prepared neuronal cultures. K.E.R. performed Western blotting. K.R.V. performed drebrin-EB3 immunoprecipitation. M.M.M. and E.W.D. wrote the manuscript.

Abstract

Synaptic communication has been clearly demonstrated to regulate microtubule (MT) dynamics in dendrites of mature neurons. Importantly, this encompasses the transient polymerization of MTs from the dendritic shaft into spines. We have previously demonstrated that these “invasions” preferentially target active synapses. MTs dwell within dendritic spines for seconds to minutes, and during these events they facilitate cargo transport by plus end-directed motor proteins. This transport is important for long-term potentiation (LTP), as inhibiting MT invasions prevents sustained morphological plasticity following its induction. Calcium influx following synaptic activity causes major changes in spine actin structure and content. This rapid actin polymerization is necessary and sufficient for MT entry into spines, but precisely which and how intermediate binding proteins facilitate actin-MT interaction in this process remains the subject of active inquiry. Of particular interest is drebrin, an actin-binding protein which is localized to dendritic spines and, in our hands, is a positive regulator of invasions. Literature suggests that the MT plus tip protein (+TIP) EB3 associates with drebrin and is necessary for normal neuronal development, though precisely how remains mechanistically opaque. The primary goal of this work has been to determine whether direct interaction between EB3 and drebrin is a primary guiding factor for MT entry into dendritic spines. To test this we employed a combination of genetic manipulation and high resolution live-cell microscopy with cultured hippocampal neurons. We show that drebrin’s actin binding domain, phosphorylation state, and developmental isoform influence MT invasions. Further, we show EB3 overexpression promotes invasions in an isoform-specific manner, and that deletion of EB3’s putative drebrin-binding domain diminishes invasions. Together these results indicate that both drebrin and EB proteins independently influence MT invasion of dendritic spines.

Introduction

Coordination of cytoskeletal dynamics in neurons contributes to all stages of development, plasticity and function (Dent et al., 2011; Dent 2017). Calcium-dependent capture of microtubules (MTs) by cortical actin facilitates cellular migration (Hutchins et al., 2014), and similar mechanisms governing postsynaptic actin may perform a conserved function as synaptic tags in functionally mature neurons (Redondo et al., 2011). We have previously demonstrated that the polymerization of MTs into dendritic spines of mature neurons, hereafter referred to as invasions, is a phenomenon not only promoted by global activity (Hu et al., 2008; Merriam et al., 2011), but which is specifically targeted to synaptically active spines (Merriam et al., 2013). MTs dwell within spines over spans of seconds to minutes (Hu et al., 2008) and during this time facilitate delivery of post-synaptic cargo by plus end-directed motors (McVicker et al., 2015). These changes in the molecular content of spines are necessary for long-term potentiation (LTP) and, in line with this, pharmacologically inhibiting invasions prevents sustained morphological plasticity following LTP induction by NMDA receptor activation (Merriam et al., 2013). Synaptic activity also evokes major calcium-dependent changes in spine actin structure and content (Hlushchenko et al., 2016). We have shown previously shown that increases in F-actin content in spines is both necessary and sufficient to promote invasions (Merriam et al., 2013). Although MTs and actin do not directly bind one another, their dynamics are coordinated by an ever-expanding list of intermediate binding partners (Coles and Bradke, 2015).

A notable candidate for guiding MT polymerization into spines is drebrin, the developmentally regulated brain protein, which we have demonstrated to be a strongly positive regulator of invasions (Merriam et al., 2013). Drebrin is found in two major isoforms arising from splice variation. An “embryonic” (E) isoform, which is expressed in many types of cells and tissues, and an “adult” (A) isoform, whose expression is exclusively neuronal and is upregulated

as neurons mature (Kojima et al.,1993, Peitsch et al., 1999, Keon et al., 2000; Jin et al. et al., 2002; Aoki et al. et al., 2005). Drebrin appears to interact with the MT plus tip protein (+TIP) EB3 in an isoform specific manner (Geraldo et al., 2008; Bazellières et al., 2012; Worth et al., 2013). It has been reported this requires an intermediate region of EB3 just preceding its C-terminal EB homology domain (Geraldo et al., 2008), and is enhanced by drebrin S142 phosphorylation by cyclin-dependent kinase 5 (Cdk5) (Worth et al., 2013). In spite of its name, Cdk5 continues to serve important functions in post-mitotic neurons (Shah and Lahiri 2014) and, by way of CaMKII (Dhavan et al., 2002), could reasonably mediate this interaction downstream of synaptic calcium influx.

Based on these and other data we investigated whether interaction between EB3 and drebrin coordinate actin and MT dynamics to promote spine invasion. Here we report that the actin binding domain of drebrin, its S142 phosphorylation state and the developmental isoform of the protein influence MT invasions. Additionally, we show that overexpression of EB3, but not EB1, increases invasion rates and deletion of the putative drebrin-binding domain within EB3 diminishes invasions. In total, these observations highlight the important contributions of both EB3 and drebrin to spine invasions, and support working models wherein their coordination following synaptic activity promotes invasions. Finally, we propose future experiments which will provide additional mechanistic insight.

Materials and Methods

Plasmids and cloning.

Gene modification (both mutations and generation of WT isoforms) was carried out by whole-plasmid PCR mutagenesis. Briefly, primers were designed with ~18-22 nucleotides (NT) complementary to plasmid on the 3' side and 15-20 NTs complementary 5' sequences. The 5' complement flanked the desired DNA insertion or substitution, or for deletions simply omitted NT present in template. A standard reaction containing 25uL Q5 2x master mix (NEB), 10ng template plasmid, and 2.5uM forward and reverse primers was diluted with PCR grade water up to 50uL. This mixture was pipetted gently, centrifuged briefly and thermocycled according to specifications for Q5 polymerase. Mutagenized plasmid DNA was purified with Monarch PCR Cleanup kit (NEB), then treated for 30 minutes with 1uL DpnI in CutSmart buffer to digest methylated template DNA. DpnI was heat-inactivated at 80°C following digestion and 5ul was immediately transformed into chemically competent bacteria (E.Cloni, Lucigen) following manufacturer guidelines. Results were confirmed by Sanger sequencing (QuintaraBio). Phosphomimetic (S142D) and non-phosphorylatable (S142A) drebrin E constructs were kind gifts from the Gordon-Weeks lab (King's College, London, UK).

Cell Culture and Transfections.

All procedures were approved by the University of Wisconsin Committee on Animal Care and were in accordance with the NIH guidelines. Primary hippocampal neurons were prepared from Sprague Dawley rats (Harlan) at E18.5 (McVicker et al., 2016). Briefly, rat hippocampi were dissected, trypsinized and transfected with plasmid DNA while in suspension using the Amaxa Nucleofector, per manufacturer instructions. Neurons were plated at a density of $3x10^4$ neurons

per cm^2 on 0.001 mg/ml PEI (Sigma)-coated coverslips, which were adhered to 35 mm plastic culture dishes containing a 15 mm hole drilled through the chamber. Neurons were plated with plating media (PM; neurobasal media with 5% fetal bovine serum (FBS), B27 supplement, 2 mM glutamine, 0.3% glucose and 37.5 mM NaCl) for 1 h at 5.0% CO^2 and 37°C, after which the chambers were flooded with 2 ml of serum-free media (PM with no added FBS). For tet-ON promoter induction 1ug/uL doxycycline was maintained in culture media for 7 days prior to imaging.

Microscopy, image processing and analysis.

Time-lapse images of live cultures were acquired either on a Nikon TE2000E microscope with total internal reflection fluorescence (TIRF) illuminator (Nikon) and Evolve EMCCD camera (Photometrics) with 100x/1.4NA objective or a Zeiss LSM800 scanning confocal system with 63x/1.4NA objective. During time-lapse microscopy, neurons were kept at 37°C in a chamber enclosing the microscope. The imaging chamber was fitted with a glass ring and sealed with silicone grease and a glass coverslip to maintain appropriate CO2 levels. Time-lapse images were acquired every 5 seconds and spanned 10 minutes per neuron. All image processing and quantification was carried out in Fiji (Schindelin et al., 2012). Depending on experimental parameters MTs were visualized by fluorescent tubulin, EB1 or EB3. Secondary and tertiary branches of hippocampal pyramidal cells were selected preferentially. Invasions were manually quantified by frame-by-frame scrutiny of time-lapse images and supported by kymographs. The percentage of spines invaded was determined by dividing the number of invaded spines over the imaging period by the total number of spines in the dendritic field. Invasion frequency was defined by the total number of invasions divided by the number of spines invaded.

Graphing and statistics

Graphpad Prism was used for all graphing and statistical analyses. For all data comparing more than two conditions, a one-way analysis of variance and Tukey's post hoc tests were performed. For data comparing only two conditions, a Student's t-test was performed. Data with P values less than 0.05 were considered statistically significant. On all graphs *P<0.05, **P<0.01 and ***P<0.001, ****P<0.0001. Cells analyzed were collected from a minimum of three preparations.

Results

Overexpression of EB family proteins differentially impact MT invasions of spines

End-binding (EB) proteins are canonical MT +TIP proteins. They are comprised of three family members, EB1, EB2 and EB3, however, only EB1 and EB3 function to bind to the polymerizing ends of MTs in neurons to promote persistent microtubule growth (Komarova et al., 2009). EB1 and EB3 share all of the same domains **(Fig. 1A)** and are often used interchangeably for "marking" growing MT +ends (Stepanova et al., 2003). However, in hippocampal neurons EB proteins show distinct temporal patterns of expression **(Fig. 1B)**. Levels are initially comparable, but EB1 expression decreases around 7DIV, whereas EB3 expression remains uniformly high. This suggests that EB3 is the predominant form in mature neurons (>18DIV) and could have a synergistic effect on MT invasions. To test whether levels of EB proteins upregulate invasions in mature neurons we overexpressed EB1-RFP or EB3-RFP and compared them to a tubulin-GFP control condition. These neurons were co-transfected with GFP or RFP volume markers to visualize spines, respectively. Relative to the tubulin controls, we observed that overexpression of EB3-RFP increased the proportion of spines targeted by MTs (193% of baseline, 24.5%±2.3, p=0.0006) **(Fig. 1D)**, as well as the frequency of invasion events (345% of baseline, 2.4±0.7, p=0.0199) **(Fig. 1E)**. In contrast, EB1 overexpression decreased the proportion of spines invaded (41% of baseline, 5.2%±1.1, p=0.025), but did not significantly diminish invasion frequency (52% of baseline, 0.4±0.1, p=0.8326) **(Figs. 1D,E)**. This is, however, significantly fewer invasions events compared to EB3 overexpression (p=0.0086). Both EB1 and EB3 labeled similar numbers of MTs in the dendrite shaft **(Fig. 1C)**, indicating the difference in invasions was not due to differential labeling of dendritic MTs. These results are significant because they indicate that EB1 and EB3 are not interchangeable "markers" of MT polymerizing ends, but actually can influence MT behavior in opposing ways.

Overexpression of developmentally regulated drebrin splice isoforms differentially impact MT invasions of spines

Drebrin (developmentally regulated brain protein) is found in two major isoforms arising from splice variation (Kojima et al., 1993). The two isoforms of drebrin include an "embryonic" (E) isoform, which is expressed in many types of cells and tissues, and an "adult" (A) whose expression is exclusively neuronal, and is upregulated as neurons mature **(Fig. 2A)**. The adult isoform contains an extra "adult specific" domain (residues 321-365) without defined function. Precise crystal structure determination of drebrin is elusive as its C-terminal is intrinsically disordered, while its N-terminal is predicted to be folded. The N-terminal domain (residues 1-133) of drebrin is critical for actin binding and modifying properties, containing an ADF homology domain (Ishikawa et al., 2017). Residues 233-317 of drebrin are critical for its binding to F-actin (Hayashi et al., 1999). Drebrin A contains two putative SxIP sequences, which are canonical sequences for binding EB proteins (Slep and Vale 2007; Honnappa et al., 2009), whereas Drebrin E has only one.

In previous experiments we showed that drebrin is capable of increasing MT invasions of spines (Merriam et al., 2013). However, this study only used the adult isoform of drebrin. We wondered if there was some heretofore unappreciated contribution of the adult splice variant in upregulating MT invasion during neuronal maturity. To test this, we directly compared invasion rates of neurons overexpressing drebrin A-GFP and drebrin E-GFP to a GFP expressing control **(Fig. 2B)**. Consistent with previous observations, overexpression of the drebrin A increased the proportion of spines invaded relative to controls by 279% (24.6%±4.5, p=<0.0001). In contrast, overexpression of the drebrin E only modestly increased proportion of spines invaded (127% baseline, 11.2%±2.0, p=0.4965). Thus, the adult isoform of drebrin is a more potent regulator of spine invasions than its earlier-expressed counterpart. These results are similar to results with

EB proteins insofar as EB3, which is expressed well into adulthood is a more potent stimulator of MT invasions compared to EB1, whose expression is downregulated in adulthood **(Fig. 1)**.

Association of drebrin with actin and the phosphorylation state of drebrin impact MT invasions

Synaptic activity evokes major calcium-dependent changes in actin structure and content within spines (Hlushchenko et al., 2016). Moreover, actin polymerization is both necessary and sufficient to promote microtubule (MT) invasion of dendritic spines (Merriam et al., 2013). Actin-MT coordination requires intermediate proteins (Coles and Bradke, 2015) and literature suggests that drebrin, a spine-enriched actin-binding protein, binds the MT +TIP protein EB3 (Geraldo et al., 2008; Bazellières et al., 2012). In our hands, drebrin expression is positively correlated with invasions (Merriam et al., 2013). Based on these observations, we hypothesized that drebrin-EB3 association serves as a transient linker to guide MT polymerization into synaptically active spines.

If drebrin serves to transiently crosslink spine actin and MT + ends, then its proper localization to and anchoring within spines should be mandatory to promote invasions. To test this hypothesis we compared invasion rates in neurons overexpressing WT drebrin and drebrin lacking these residues (drebrin-ΔABS) to a GFP volume marker as a control condition **(Fig. 3)**. Wild-type (WT) drebrin-GFP overexpression specifically labeled dendritic spines **(Fig. 3A)** and increased both the proportion of spines targeted by MTs by 297% (25.2%±3.2, $p<0.0001$) **(Fig. 3C)** and the frequency of invasions by 445% (5.0±0.8, $p<0.0001$) **(Fig. 3D)**, compared to GFP controls. In contrast, drebrin-ΔABS was strikingly diffuse in appearance compared to WT drebrin-GFP **(Fig. 3B)**. Relative to controls, drebrin-ΔABS overexpression decreased invasion frequency by 57% (0.5±0.2, $p=0.2965$) and the proportion of spines targeted by 62% (3.2%±0.2, $p=0.0696$) **(Figs. 3C, D)**. Therefore, increasing total drebrin expression does not promote

invasions unless it is able to bind F-actin, and properly localizes to spines. Further, the drebrin-ΔABS mutant appears to exert dominant-negative interference, possibly by competing for interactors.

Others have reported that phosphorylation of drebrin S142 by Cdk5 regulates its interaction with EB3, where the addition of a negative charge at this site is permissive and its absence is inhibitory (Worth et al., 2013). To test whether drebrin S142 phosphorylation influences spine invasion we overexpressed GFP-tagged phospho-mimetic (S142D) and non-phosphorylatable (S142A) drebrin E mutant constructs (Worth et al., 2013), in hippocampal neurons. We used drebrin E instead of drebrin A because we reasoned that drebrin A overexpression may already cause maximum MT invasions, so we might not detect an increase with the phospho-mutants. Overexpression of drebrin E-S142D only modestly increased the proportion of spines targeted (149% of baseline, 18.3%±3.7, $p=0.1597$) but significantly promoted invasion frequency by 222% (2.6±0.6, $p=0.0237$). Overexpression of drebrin E-S142A exhibited a trend toward decreasing the proportion of spines invaded, but did not reach statistical significance (46% of baseline, 5.7%±1.4, $p=0.1406$). The frequency of invasions in drebrin E-S142A expressing neurons was not significantly reduced relative to controls (71% of baseline, 0.8±0.3, $p=0.7846$), but was significantly lower than the phospho-mimetic S142D variant ($p=0.012$). These results suggest that phosphorylation of S142 in drebrin regulates its function with regard to MT invasions of spines.

Removal of the putative drebrin-binding motif in EB3 affects MT invasions

It has been reported that drebrin binds EB3, but not EB1, and serial fragmentation and immunoprecipitation suggests EB3 residues 177-194 are necessary for this interaction (Geraldo et al., 2008). To test whether the the putative drebrin-binding site suggested by Geraldo et al.

contributes to invasions we generated an EB3Δi “intermediate” (AA 177-194) deletion mutant, specific to the region of no other ascribed function preceding the C-terminal EB homology domain **(Fig. 1A)**. However, since EBs naturally hetero- and homo-dimerize (Slep and Vale 2007), potential masking of effect by WT background expression was of major concern. Further, this manipulation should be delayed until maturity to preserve early development, given the broad contributions of EBs during this period (van de Willige et al., 2016). Finally, having illustrated that EB3 overexpression promotes invasion, best practices would keep total protein at physiologically relevant levels.

To address these technical concerns we developed a novel, inducible knockdown-rescue (KDR) vector to delay gene replacement until functional maturity. The development of this approach and requisite materials are detailed at length in Chapter 3. Briefly, our single-transcript approach temporally locks delivery of the gene of interest-targeting miRNA with expression of a “rescue” gene, under the control of a tet-ON promoter. In mature hippocampal neurons induced for KDR of endogenous EB3 with WT EB3-RFP we observed 22.7%±2.3 of spines invaded **(Fig. 5A)**. In contrast EB3Δi KDR caused a decrease of 22% from this baseline (17.8%±1.8, p=0.0498, n=24). This result suggests that the intermediate region in EB3 serves a previously undocumented role in MT invasion of spines.

Elimination of drebrin SxIP sequences has no impact on invasions

While significant and consistent, the modest decrease in spines invaded in EB3Δi KDR clearly indicates that additional mechanisms contribute to spine invasion. If invasions are crucial for delivering postsynaptic cargo (McVicker et al., 2016) we should expect considerable functional redundancy. One means of accomplishing this, and a distinct possibility could be additional binding sites between EB3 and drebrin. To date, no EB3 binding motifs or regions are

defined within drebrin and, if proven to be direct, EB3 residues 177-194 represent a highly unconventional mode of interaction. Most proteins that associate with EB family proteins do so by virtue of SxIP motifs, colloquially referred to as +TIP localization sequences (Honnappa et al., 2009). We noted that drebrin has two unvalidated SxIP sequences, one SSLP and one TPIP, which, if legitimate, would represent a novel means of interacting with +TIPs **(Fig. 2)**. To test whether these putative SxIP motifs in drebrin promote invasion by association with EB3 we mutated both, to generate a drebrin A ΔSxIP-RFP (SSLP→SSAA, TPIP→TPAA substitution) construct, and again applied our KDR technique. However, in mature hippocampal neurons we detected no contribution of these motifs toward invasions. KDR of WT drebrin averaged 17.7%±3.1 (n=17) of spines invaded, while Drebrin ΔSxIP averaged 20.0%±2.6 (n=17, p=0.576) **(Fig. 5B)**. It is therefore unlikely that SxIP sequences within drebrin are valid functional motifs.

In an effort to confirm that drebrin and EB3 immunoprecipitate together in neurons, as has been shown in COS-7 cells (Geraldo et al., 2008) we overexpressed HA-labeled drebrin A in neurons. Immunoprecipitation of HA-drebrin A followed by Western blotting for EB3 did not yield any co-IP of these two proteins, under the same conditions that did co-IP actin **(Fig. 6)**. All together, these results suggest that EB3 and drebrin A both serve important functions in helping guide polymerizing MTs into dendritic spines. Nevertheless, none of the data that has been collected in mature neurons indicates EB3 and drebrin are functioning as proteins that directly interact with one another to promote MT invasion of spines.

Discussion

Changes in the structure, organization, and molecular composition of dendritic spines precede and are necessary for sustained expression of long-term potentiation (LTP) (Xu et al., 2009; Yang et al., 2009; Hubener and Bonhoeffer, 2010). A lingering question in the field of neuroscience has been how these materials are efficiently delivered to support spines undergoing plasticity. Previously, both passive and active transport models have been proposed (Guillaud et al., 2008; Ryan et al., 2005; Desnos et al., 2007; Correia et al., 2008) but are lacking in terms of specificity. Many components of the postsynaptic density (PSD) must be shuttled along microtubules (MTs) from the soma and through dendrites by molecular motors (Verhey et al., 2011; Cianfrocco et al., 2015). We recently demonstrated that a direct-deposit scheme facilitated by transient MT invasion supplies postsynaptic cargo into specific dendritic spines (McVicker et al., 2016). These invasions are necessary for sustained morphological plasticity following NMDA receptor activation (Merriam et al., 2011). Moreover, activity-dependent changes in spine F-actin determine which spines are invaded (Merriam et al., 2013). These observations support a long-postulated “synaptic tagging and capture” model (Redondo and Morris 2011). Here we hypothesize that changes in actin and actin-associated proteins “tag” which individual spines require material support, and delivery of cargo by MT motors to “capture” the expression of LTP by active synapses. Although, how and which tubulin- and actin-associated intermediate proteins coordinate this process remains unknown.

Literature suggests that key processes in developing neurons rely on interaction between the MT +TIP protein EB3 and actin-binding protein drebrin (Geraldo et al., 2008, Worth et al., 2013; Sonego et al., 2015; Ketschek et al., 2016). In the present study we investigated whether these proteins share conserved functions in the synaptic plasticity of mature cultured hippocampal neurons. We report that EB3 overexpression increases both the frequency of

spine invasion events (345%) as well as the proportion of spines targeted (193%) compared to GFP-tubulin expressing controls. In contrast, overexpression of EB1, which has been reported not to interact with drebrin (Geraldo et al., 2008), significantly decreases both of these same metrics (52% frequency, 41% proportion). We show here that in cultured hippocampal neurons, EB1 levels decrease after 7 DIV, while EB3 levels remain consistently high during development and throughout maturity, which is consistent with previous studies (Jaworski et al., 2009). Given that EB1 and EB3 readily heterodimerize (Slep and Vale 2007), an explanation consistent with previous observations is that elevated EB1 levels behave in a dominant-negative fashion by outcompeting and displacing endogenous EB3 in mature neurons, thus decreasing the likelihood for MTs to be guided into spines by drebrin. In support of this, knockdown-rescue (KDR) induced in mature neurons replacing endogenous EB3 with mutant EB3 lacking its putative drebrin-binding interface (EB3Δi, residues 177-194) (Geraldo et al., 2008) diminished the proportion of spines invaded by 23%.

While the EB3-interacting site within drebrin has not been identified, its affinity for EB3 is reportedly governed by the phosphorylation state of the S142 residue via cyclin-dependent kinase 5 (Cdk5) (Worth et al., 2013). When we overexpressed phosphomimetic S142D drebrin E we found that the frequency of MT invasions was increased compared to WT drebrin E (222%) and the non-phosphorylatable S142A drebrin E mutant (315%). Moreover, the proportion of spines invaded was greater than the non-phosphorylatable S142A drebrin E mutant (322%), but was not significantly different than WT drebrin E. Cdk5 remains present and necessary in mature neurons (Shah and Lahiri, 2014) and could reasonably phosphorylate drebrin as part of a CaMKII-dependent signaling cascade activated by synaptic calcium influx (Dhavan et al., 2002; McVicker et al., 2015). It should be noted that the influence of drebrin S142 phosphorylation on EB3 affinity is, at present, experimentally inextricable from its effects

on F-actin, considering phosphorylation of this site is also reported to reveal cryptic actin bundling activity (Worth et al., 2013). As we have previously demonstrated that F-actin structure and content itself is fundamental in guiding MTs into spines, it will be difficult to determine which of these synergistic invasion-promoting functions of drebrin, either phosphorylation or exposure of an F-actin binding motif, is more important.

Toward this end, we also report that actin-binding deficient drebrin (ΔABS) is incapable of promoting invasions in the manner of WT drebrin. This indicates that both proper localization of drebrin to spines and its ability to interact with F-actin are mandatory in this process. In fact, drebrin ΔABS may behave in dominant-negative fashion, presumably competing for binding partners which would normally contribute to invasions. Recently developed pharmacological agents may be applied toward these questions in future experiments. An interesting complementary study could employ 3,5-bis(trifluoromethyl)pyrazole (BTP), an anti-metastatic drug which is now understood to bind drebrin and sterically hinder it from modifying F-actin (Mercer et al. 2010). This study clearly illustrates that BTP prevents overexpressed drebrin from inducing aberrant filopodia formation in immortalized cells, but does not appear to reduce overlapping staining with phalloidin. Considering this, BTP might provide a powerful means of teasing apart whether drebrin predominantly exerts effects on invasions via F-actin polymerization, if its localization and function as an actin-MT crosslinker is most important, or if other important contributions remain undiscovered. Finally, on this note, we also demonstrate that drebrin E lacks the potency of its adult splice variant in guiding MTs into dendritic spines. This is entirely in line with past demonstrations that drebrin A-null mice specifically exhibit deficiencies in hippocampal LTP and adult learning and memory (Kojima et al, et al., 2010; Kojima et al., 2016). Mechanistic explanation for this will require additional careful study, as a chicken-or-the-egg situation arises. Regardless, in combination with developmental expression

trajectories of EB1 and EB3, these data suggest this mode of targeting materials to spines becomes more prevalent in mature neurons.

Future research will also be needed to evaluate whether EB3 residues 177-194 indeed function as an unconventional binding motif, and to rule out the possibility that truncation has deleterious physical consequences unrelated to direct binding. Chimeric constructs swapping the region deleted in EB3Δi with the corresponding residues from EB1, and vice versa will be illuminating. If truncation alone is responsible, restoring full length to EB3 by inserting residues from should also restore invasions. However, if EB3 directly binds drebrin in an isoform specific manner, we should expect the chimeric protein to behave as its donor isoform. Additionally, it is entirely possible that other isoform-specific features contribute to the differences observed between EB1 and EB3. Notably, natural selectivity of +TIP complexes with preference for one isoform over the other (Ferreira et al., 2013; Leśniewska et al., 2014) could differ in their ability to guide invasions. Since, canonically, EB-associated proteins bind to the EB-homology region of its C-terminal region, chimeric C-terminal swap chimeras could be employed to test this possibility. If isoform-specific differences in +TIP complexes contribute in any way to invasions, we expect, based on data from the present study, that either chimera would reflect its donor isoform. From here, determining which additional intermediate proteins may be involved would be of great interest.

Though additional careful research is required to understand the precise mechanistic contributions of EB3 and drebrin in promoting invasions, these observations highlight the importance of both proteins in this process, and support working models wherein their coordination, following synaptic activity, selectively facilitates cargo delivery to support spines undergoing plasticity.

References

Aoki C, Sekino Y, Hanamura K, et al. Drebrin A is a postsynaptic protein that localizes in vivo to the submembranous surface of dendritic sites forming excitatory synapses. J Comp Neurol. 2005;483(4):383-402.

Bazellières E, Massey-harroche D, Barthélémy-requin M, Richard F, Arsanto JP, Le bivic A. Apico-basal elongation requires a drebrin-E-EB3 complex in columnar human epithelial cells. J Cell Sci. 2012;125(Pt 4):919-31.

Cianfrocco MA, Desantis ME, Leschziner AE, Reck-peterson SL. Mechanism and regulation of cytoplasmic dynein. Annu Rev Cell Dev Biol. 2015;31:83-108.

Coles CH, Bradke F. Coordinating neuronal actin-microtubule dynamics. Curr Biol. 2015;25(15):R677-91.

Correia SS, Bassani S, Brown TC, et al. Motor protein-dependent transport of AMPA receptors into spines during long-term potentiation. Nat Neurosci. 2008;11(4):457-66.

Dent EW, Gupton SL, Gertler FB. The growth cone cytoskeleton in axon outgrowth and guidance. Cold Spring Harb Perspect Biol. 2011;3(3)

Dent EW. Of microtubules and memory: implications for microtubule dynamics in dendrites and spines. Mol Biol Cell. 2017;28(1):1-8.

Desnos C, Huet S, Darchen F. 'Should I stay or should I go?': myosin V function in organelle trafficking. Biol Cell. 2007;99(8):411-23.

Dhavan R, Greer PL, Morabito MA, Orlando LR, Tsai LH. The cyclin-dependent kinase 5 activators p35 and p39 interact with the alpha-subunit of Ca2+/calmodulin-dependent protein kinase II and alpha-actinin-1 in a calcium-dependent manner. J Neurosci. 2002;22(18):7879-91.

Ferreira JG, Pereira AJ, Akhmanova A, Maiato H. Aurora B spatially regulates EB3 phosphorylation to coordinate daughter cell adhesion with cytokinesis. J Cell Biol. 2013;201(5):709-24.

Geraldo S, Khanzada UK, Parsons M, Chilton JK, Gordon-weeks PR. Targeting of the F-actin-binding protein drebrin by the microtubule plus-tip protein EB3 is required for neuritogenesis. Nat Cell Biol. 2008;10(10):1181-9.

Guillaud L, Wong R, Hirokawa N. Disruption of KIF17-Mint1 interaction by CaMKII-dependent phosphorylation: a molecular model of kinesin-cargo release. Nat Cell Biol. 2008;10(1):19-29.

Hlushchenko I, Koskinen M, Hotulainen P. Dendritic spine actin dynamics in neuronal maturation and synaptic plasticity. Cytoskeleton (Hoboken). 2016;73(9):435-41.

Honnappa S, Gouveia SM, Weisbrich A, et al. An EB1-binding motif acts as a microtubule tip localization signal. Cell. 2009;138(2):366-76.

Hu X, Viesselmann C, Nam S, Merriam E, Dent EW. Activity-dependent dynamic microtubule invasion of dendritic spines. J Neurosci. 2008;28(49):13094-105.

Hübener M, Bonhoeffer T. Searching for engrams. Neuron. 2010;67(3):363-71.

Hutchins BI, Wray S. Capture of microtubule plus-ends at the actin cortex promotes axophilic neuronal migration by enhancing microtubule tension in the leading process. Front Cell Neurosci. 2014;8:400.

Jaworski J, Kapitein LC, Gouveia SM, et al. Dynamic microtubules regulate dendritic spine morphology and synaptic plasticity. Neuron. 2009; 61(1):85-100.

Jin M, Tanaka S, Sekino Y, et al. A novel, brain-specific mouse drebrin: cDNA cloning, chromosomal mapping, genomic structure, expression, and functional characterization. Genomics. 2002;79(5):686-92.

Keon BH, Jedrzejewski PT, Paul DL, Goodenough DA. Isoform specific expression of the neuronal F-actin binding protein, drebrin, in specialized cells of stomach and kidney epithelia. J Cell Sci. 2000;113 Pt 2:325-36.

Ketschek A, Spillane M, Dun XP, Hardy H, Chilton J, Gallo G. Drebrin coordinates the actin and microtubule cytoskeleton during the initiation of axon collateral branches. Dev Neurobiol. 2016;76(10):1092-110.

Kojima N, Hanamura K, Yamazaki H, Ikeda T, Itohara S, Shirao T. Genetic disruption of the alternative splicing of drebrin gene impairs context-dependent fear learning in adulthood. Neuroscience. 2010;165(1):138-50.

Kojima N, Shirao T, Obata K. Molecular cloning of a developmentally regulated brain protein, chicken drebrin A and its expression by alternative splicing of the drebrin gene. Brain Res Mol Brain Res. 1993;19(1-2):101-14.

Kojima N, Yasuda H, Hanamura K, Ishizuka Y, Sekino Y, Shirao T. Drebrin A regulates hippocampal LTP and hippocampus-dependent fear learning in adult mice. Neuroscience. 2016;324:218-26.

Komarova Y, De groot CO, Grigoriev I, et al. Mammalian end binding proteins control persistent microtubule growth. J Cell Biol. 2009;184(5):691-706.

Leśniewska K, Warbrick E, Ohkura H. Peptide aptamers define distinct EB1- and EB3-binding motifs and interfere with microtubule dynamics. Mol Biol Cell. 2014;25(7):1025-36.

Mcvicker DP, Awe AM, Richters KE, et al. Transport of a kinesin-cargo pair along microtubules into dendritic spines undergoing synaptic plasticity. Nat Commun. 2016;7:12741.

McVicker DP, Millette MM, Dent EW. Signaling to the microtubule cytoskeleton: an unconventional role for CaMKII. Dev Neurobiol. 2015;75(4):423-34.

Merriam EB, Lumbard DC, Viesselmann C, et al. Dynamic microtubules promote synaptic NMDA receptor-dependent spine enlargement. PLoS ONE. 2011;6(11):e27688.

Merriam EB, Millette M, Lumbard DC, et al. Synaptic regulation of microtubule dynamics in dendritic spines by calcium, F-actin, and drebrin. J Neurosci. 2013;33(42):16471-82.

Peitsch WK, Grund C, Kuhn C, et al. Drebrin is a widespread actin-associating protein enriched at junctional plaques, defining a specific microfilament anchorage system in polar epithelial cells. Eur J Cell Biol. 1999;78(11):767-78.

Redondo RL, Morris RG. Making memories last: the synaptic tagging and capture hypothesis. Nat Rev Neurosci. 2011;12(1):17-30.

Ryan XP, Alldritt J, Svenningsson P, et al. The Rho-specific GEF Lfc interacts with neurabin and spinophilin to regulate dendritic spine morphology. Neuron. 2005;47(1):85-100.

Shah K, Lahiri DK. Cdk5 activity in the brain - multiple paths of regulation. J Cell Sci. 2014;127(Pt 11):2391-400.

Skube SB, Chaverri JM, Goodson HV. Effect of GFP tags on the localization of EB1 and EB1 fragments in vivo. Cytoskeleton (Hoboken). 2010;67(1):1-12.

Slep KC, Vale RD. Structural basis of microtubule plus end tracking by XMAP215, CLIP-170, and EB1. Mol Cell. 2007;27(6):976-91.

Sonego M, Oberoi M, Stoddart J, et al. Drebrin regulates neuroblast migration in the postnatal mammalian brain. PLoS ONE. 2015;10(5):e0126478.

van de Willige D, Hoogenraad CC, Akhmanova A. Microtubule plus-end tracking proteins in neuronal development. Cellular and molecular life sciences : CMLS. 2016; 73(10):2053-77.

Verhey KJ, Kaul N, Soppina V. Kinesin assembly and movement in cells. Annu Rev Biophys. 2011;40:267-88.

Worth DC, Daly CN, Geraldo S, Oozeer F, Gordon-Weeks PR. Drebrin contains a cryptic F-actin-bundling activity regulated by Cdk5 phosphorylation. J Cell Biol. 2013;202(5):793-806.

Xu T, Yu X, Perlik AJ, et al. Rapid formation and selective stabilization of synapses for enduring motor memories. Nature. 2009;462(7275):915-9.

Yang G, Pan F, Gan WB. Stably maintained dendritic spines are associated with lifelong memories. Nature. 2009;462(7275):920-4.

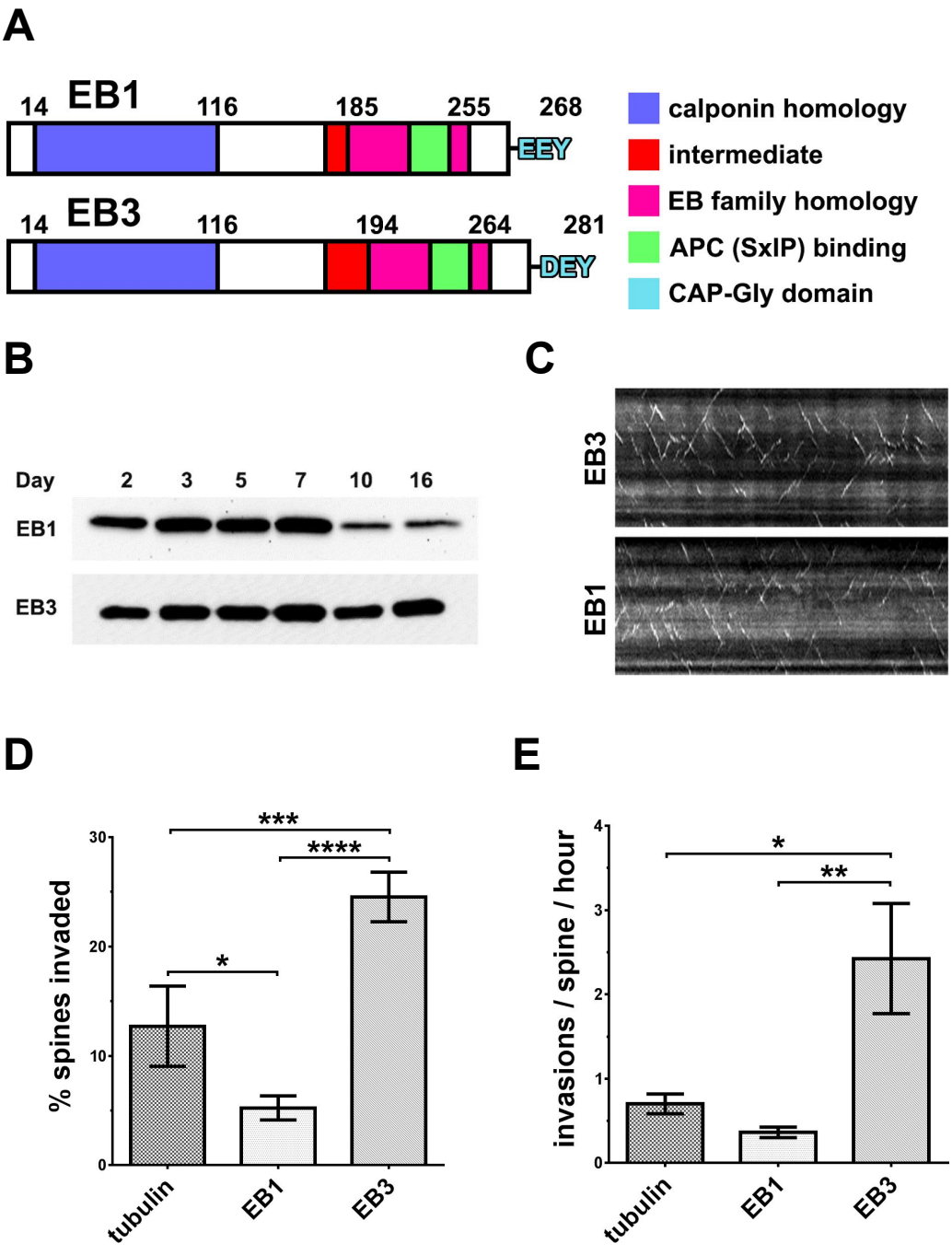
A
14
EB1
116
185
255
268
EEY
14
EB3
116
194
264
281
DEY
calponin homology
intermediate
EB family homology
APC (SxIP) binding
CAP-Gly domain
B
Day
2
3
5
7
10
16
EB1
EB3
C
EB3
EB1
D
% spines invaded
30
20
10
0
***
****
*
tubulin
EB1
EB3
E
invasions / spine / hour
4
3
2
1
0
*
**
tubulin
EB1
EB3

Fig. 1) EB1 overexpression decreases, while EB3 overexpression increases MT invasions.

(A) Diagrams of EB1 and EB3 with domains shown in different colors. Amino acid residue numbers are shown as well. (B) Expression of EB1 and EB3 in hippocampal neurons that have been cultured for various days in vitro (DIV). Note that EB1 decreases after 7DIV, while EB3 remains high to 16DIV, the earliest age that MT invasions are quantified in hippocampal cultures. (C) Kymographs from dendrites of EB1 and EB3 overexpressing neurons show no apparent difference in velocity. (D) Bar graph showing that EB1 expression decreases the percent of spines invaded significantly, while EB3 increases the percent of spines invaded significantly. EB1 proportion (41% of baseline, 5.2%±1.1, p=0.025, n=6), EB3 proportion (193% of baseline, 24.5%±2.3, p=0.0006, n=6). (E) Bar graph showing that EB1 expression decreases the frequency of MT invasion of spines slightly, while EB3 increases the frequency of invasions significantly. EB1 frequency (51.9% of baseline, 0.4±0.1, p=0.8326, n=6), EB3 frequency (345% of baseline, 2.4±0.7, p=0.0199, n=6). ANOVA with Tukey's multiple comparisons test. All graphs show mean±SEM, * p<0.05,** p<0.01, *** p<0.001, **** p<0.001.

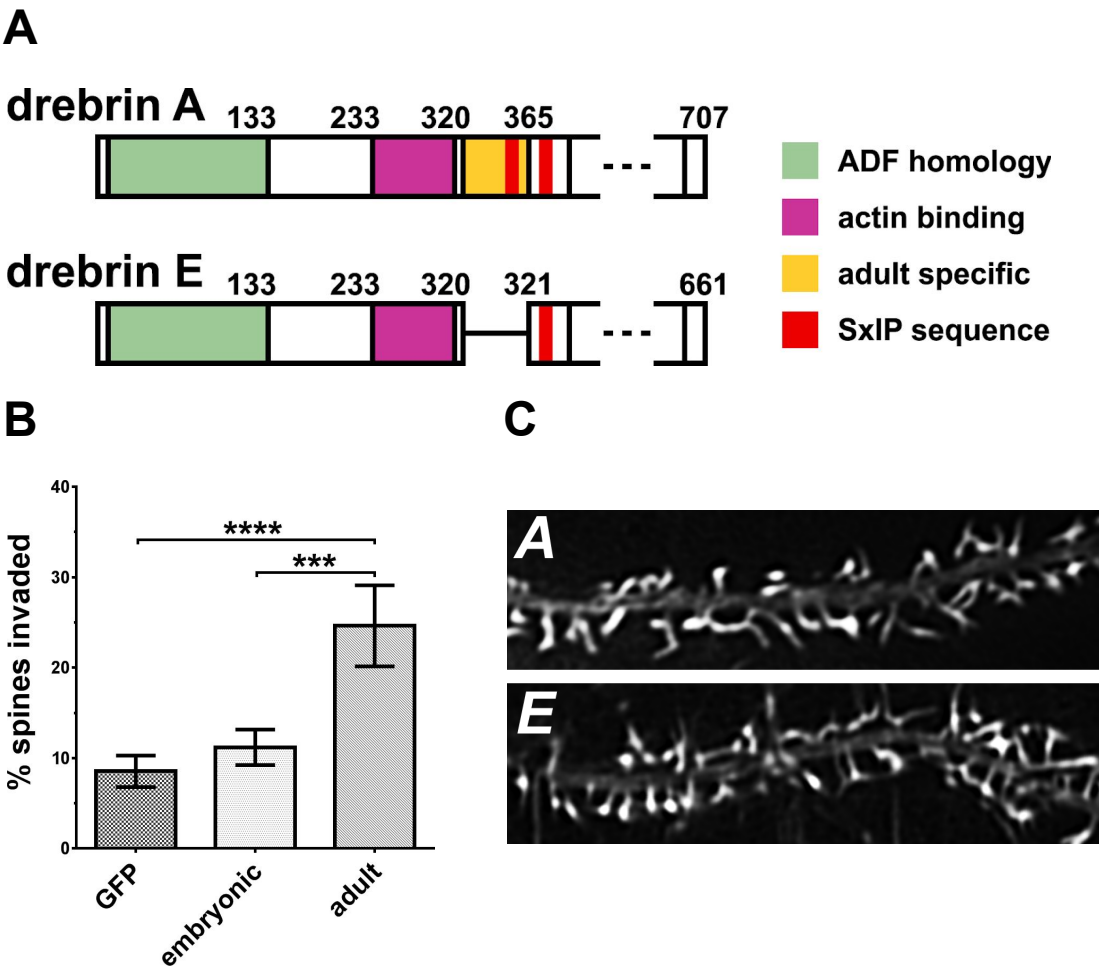

Fig. 2) Drebrin isoforms, domains and effects on MT invasion of spines.

(A) Diagrams of drebrin E (embryonic) and drebrin A (adult) isoforms are shown with domains colored and defined on the right. (B) Bar graph showing that overexpression of the embryonic drebrin (drebrin E) splice isoform does not affect MT invasion of spines, while adult drebrin (drebrin A) splice isoform affects MT invasion significantly. Drebrin E proportion (127% of baseline, 11.2%+/-2.0, p=0.4965 , n=10), Drebrin A proportion (279% of baseline, 24.6%+/-4.5, p<0.0001 , n=7). ANOVA with Tukey's multiple comparisons test. All graphs show mean±SEM, *** p<0.001, **** p<0.001. (C) Fluorescent images of drebrin A expression and drebrin E in dendrites from 20DIV hippocampal neurons.

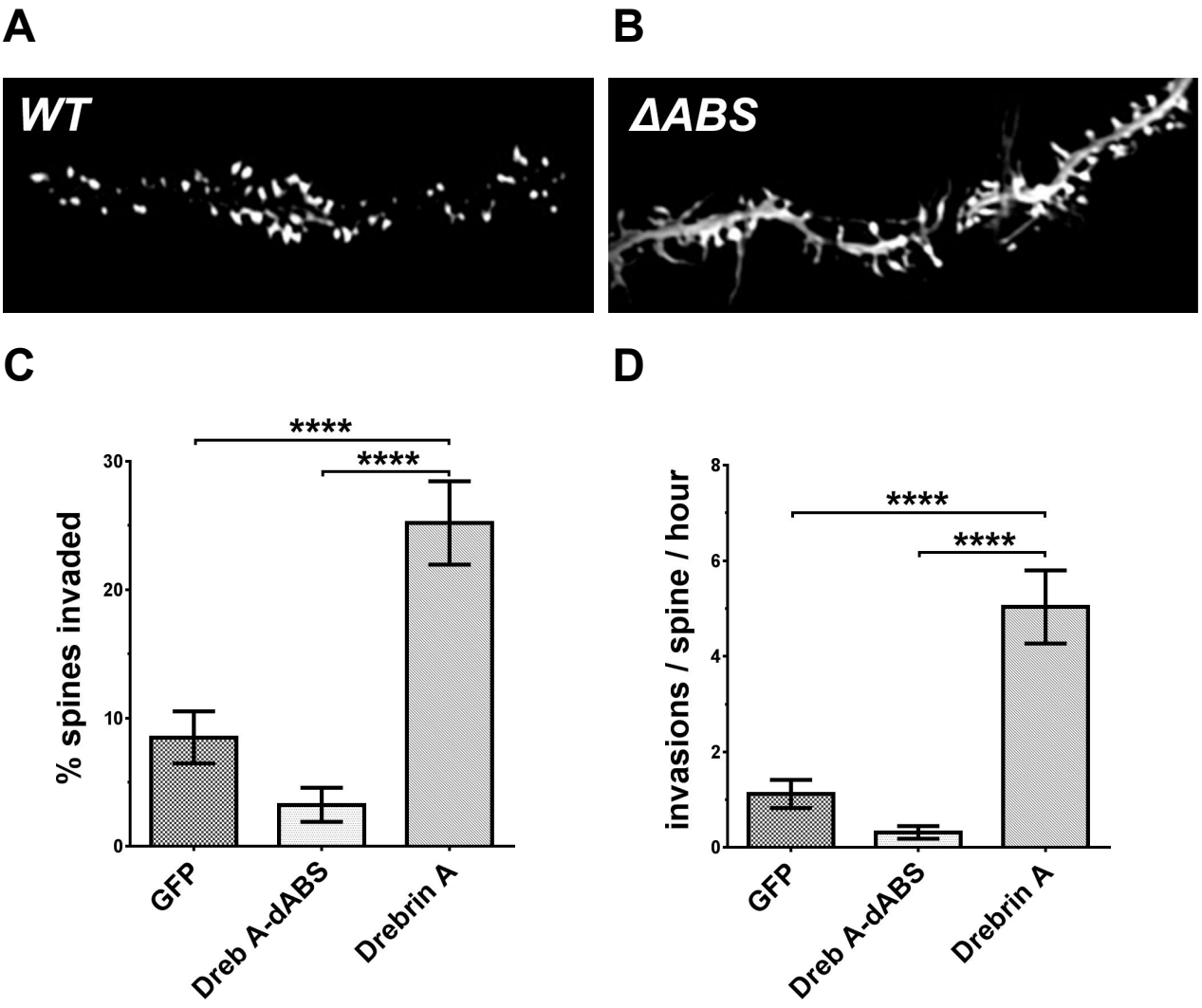

Fig. 3) Drebrin actin-binding deficient mutant reduces MT invasions of spines.

(A) Fluorescent images of wild-type drebrin A (WT) expression and (B) the drebrin A actin-binding deficient mutant (delta-ABS) in dendrites from 20DIV hippocampal neurons. (C) Bar graph showing that drebrin A delta-ABS decreases the percent of spines invaded (Drebrin A proportion (297% of baseline, 25.0%±3.2 $p<0.0001$, n=22), Drebrin dABS proportion (26% of baseline, 2.2%±0.9, $p=0.0696$, n=12) . (D) Bar graph showing that drebrin A delta-ABS decreases the invasion frequency of MTs into dendritic spines decreases (drebrin A frequency (449% of baseline, 5.0±0.8, $p<0.0001$, n=22), drebrin dABS frequency (43% of baseline, 0.5±0.2, $p=0.2965$, n=12)). ANOVA with Tukey's multiple comparisons test. All graphs show mean±SEM, * $p<0.05$, ** $p<0.01$, *** $p<0.001$, **** $p<0.001$.

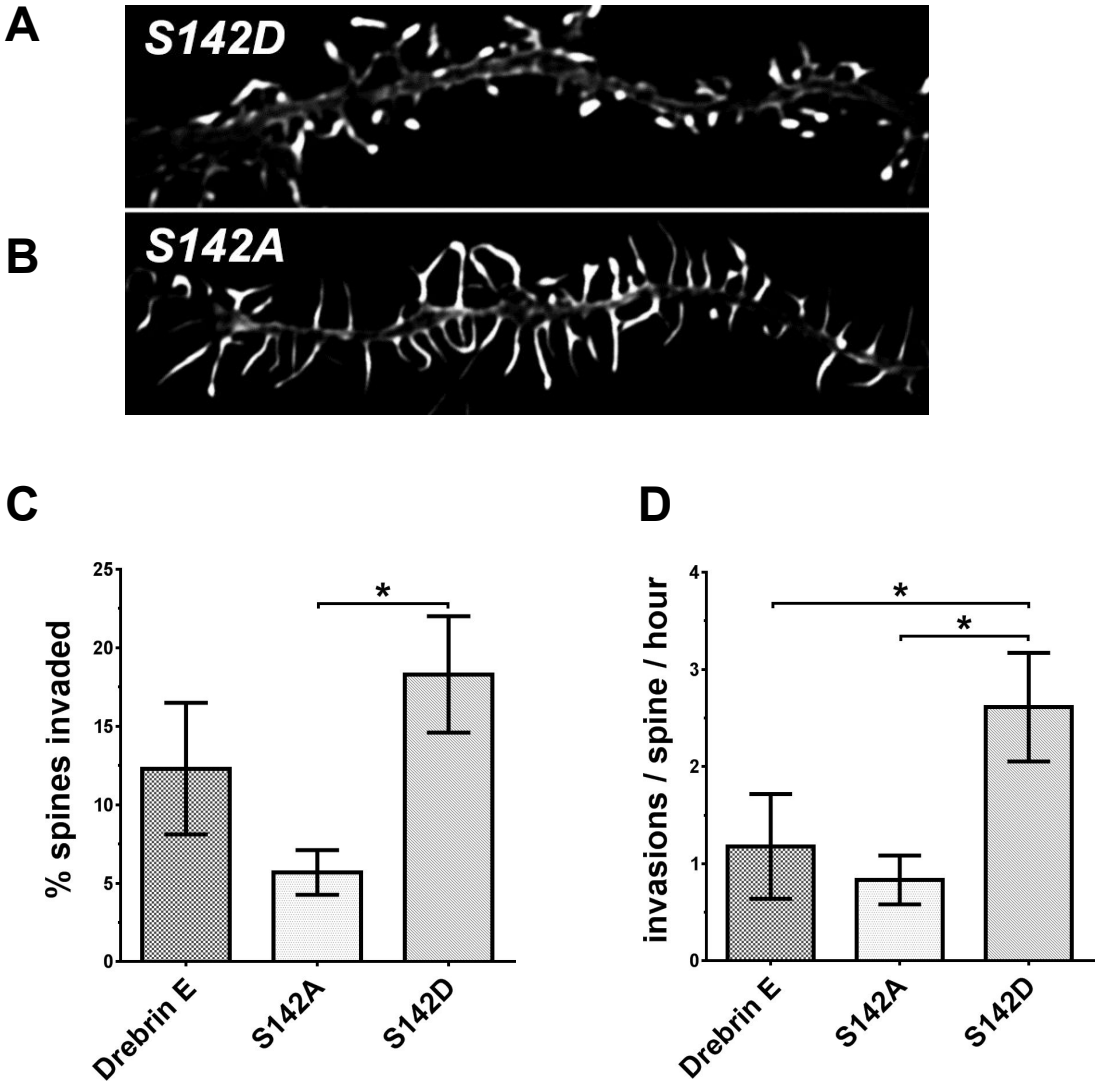

Fig. 4) Phospho-mimetic Drebrin E increases MT invasions of spines.

(A) Fluorescent images of drebrin E S142D expression and (B) drebrin E S142A in dendrites from 20DIV hippocampal neurons. (C) Bar graphs showing that drebrin S142D increases the percent of spines invaded by MTs significantly, while drebrin S142A decreases invasions slightly (drebrin E-S142A proportion (46% of baseline, 5.7%±1.4, p=0.1811, n=6), drebrin E-S142D proportion (149% of baseline, 18.3%±3.7, p=0.2042, n=5). (D) Bar graphs showing that drebrin S142D increases the frequency of spine invasions by MTs significantly, while drebrin S142A decreases invasion frequency slightly (drebrin E S142A frequency (71% of baseline, 0.8±0.3, p=0.7846, n=6, drebrin E S142D frequency (222% of baseline, 2.6±0.6, p=0.0237, n=5).

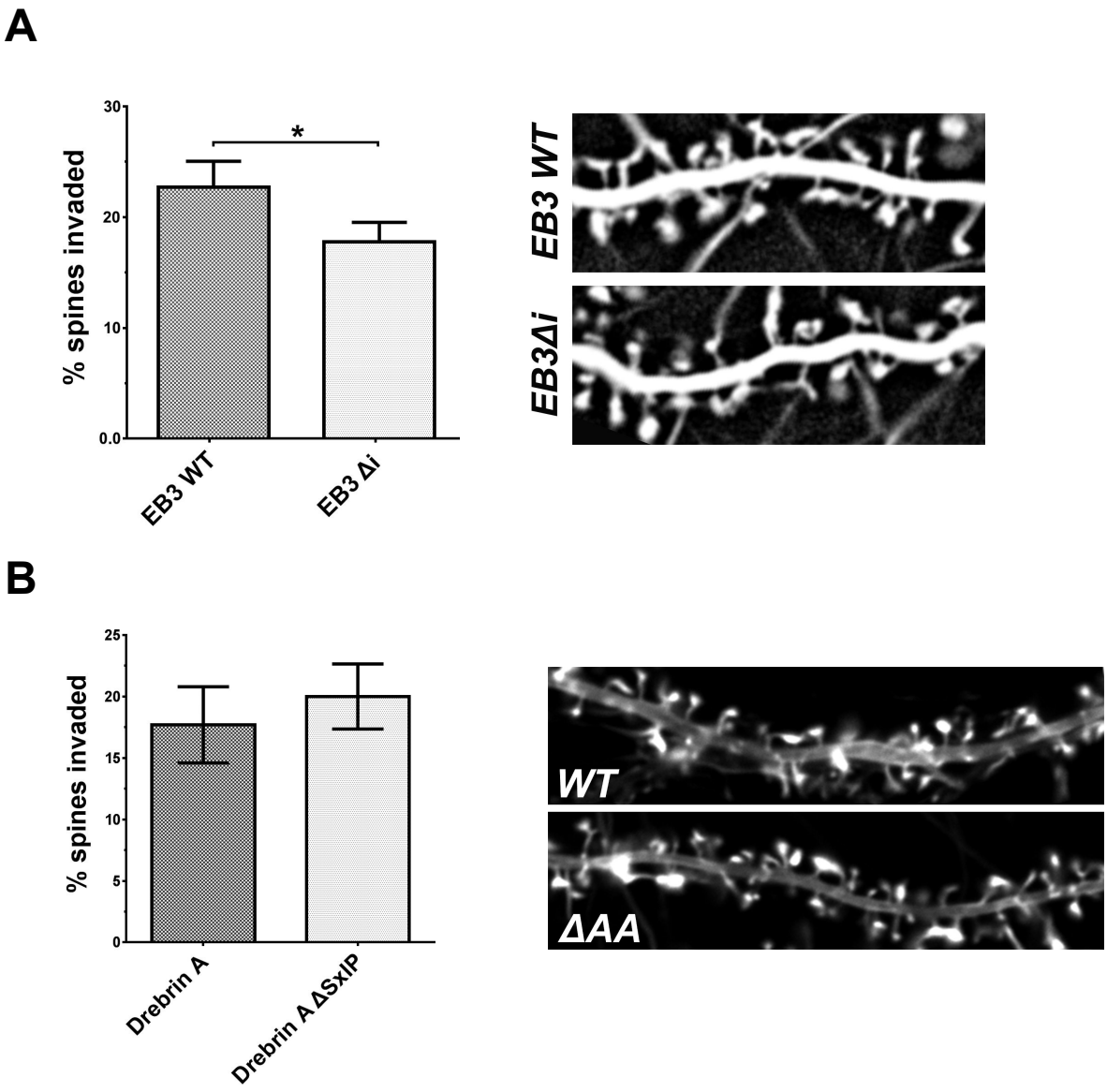

Fig. 5) EB3Δi (177-194 deletion) knockdown-rescue (KDR) decreases MT invasions, while drebrin A ΔSxIP-RFP (SSLP→SSAA, TPIP→TPAA substitution) KDR does not.

(A) Removal of putative drebrin binding region of EB3 (177-194aa deletion) decreases the percent of spines invaded by MTs significantly. EB3 (22.7%±2.3, n=26), EB3Δi (17.8%±1.8, n=24, 78% of baseline, p=0.0498). (B) Drebrin A ΔSxIP-RFP (SSLP→SSAA, TPIP→TPAA substitution) knockdown-rescue does not impact the percentage of spines invaded. Drebrin WT 17.7%±3.1 (n=17), Drebrin ΔSxIP 20%±2.6 (p=0.576, n=17). Student's T-test. All graphs show mean±SEM, * p<0.05.

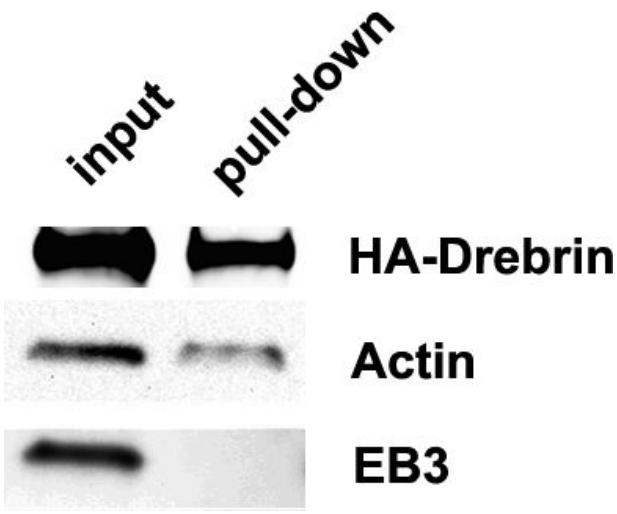

Fig. 6) Drebrin does not pull down EB3 in cortical neurons.

Under physiological conditions drebrin A does not immunoprecipitate with EB3 in cortical neurons. Actin is used as a positive control.

Chapter 3

A Novel Plasmid Toolkit for Inducible, Reversible Gene Silencing and Replacement

This work has generated a patent pending with WARF. VECTOR FOR GENE SILENCING AND REPLACEMENT AND METHODS OF USE THEREOF. 62/622479. January 26, 2018

Millette MM, Richters KE, Vogel KR, Dent EW. To be submitted.

Author contributions: M.M.M. and E.W.D. conceived the project. M.M.M. performed all cloning, imaging and analysis. M.M.M. and K.E.R. prepared neuronal cultures. K.E.R. and K.R.V. performed Western blotting. M.M.M. and E.W.D. wrote the manuscript.

Abstract

Interrogating the roles of individual proteins in complex biological processes commonly requires the expression of functional mutants in both gain- and loss-of-function experiments. However, background contribution of endogenous protein represents a primary confounding factor when interpreting the consequences of these alterations. This is particularly troublesome when proteins of interest are functionally obligate dimers or multimers. Further, when proteins of interest serve multiple functions in a system, even modest overexpression within a depleted background may obscure the effects of specific, targeted mutations by upregulating other processes. At present, the concept of a knock-down replacement strategy to study protein function has not been implemented in any methodical way. We recognized this lack of tools as opportunity to advance the field and developed a novel system to carry out complete, physiologically-matched genetic replacement of proteins of interest using an inducible, modular plasmid. Our method overcomes fundamental issues intrinsic to all currently available alternatives for primary cell transfection. At its core, this provides a platform for researchers to study effects of genetic ablation or functional mutations with a high degree of temporal control to focus on specific developmental time points. As such, the advantages of our system to neuroscience are myriad, but are broadly applicable within the realm of general cell biology. Notably, many of the challenges intrinsic to primary neuronal culture are shared with gene therapy, which remains a major hurdle in modern medicine, and may thus benefit from the same strategies. Though tools devised for basic research are rarely directly translatable to clinical application, we designed this technique to be easily portable and entirely vector agnostic. Thus, future advances in viral therapeutics may be harnessed without undue complication, enhancing, rather than antiquating, this strategy.

Introduction

Our lab has historic and ongoing focus on how cytoskeletal dynamics contribute to synaptic plasticity. Specifically, we are interested in how actin and microtubules (MTs) coordinate to direct the deposit of cargoes necessary for long-term potentiation (LTP), one of the major mechanisms that underlies learning and memory, into synaptically active dendritic spines (Dent, 2017). Though advances are being made toward generating cultured neuronal networks from induced pluripotent stem cells (IPSCs) (Lam et al., 2017), the quality and reliability of primary rodent hippocampal neurons maintains them as the well-favored model to study the cellular and molecular bases of learning and memory. The exogenous expression of genetically encoded, fluorescent fusion proteins to visualize these processes is a mainstay of this research. In culture, as *in vivo*, neurons form dense and elaborate networks. Consequently, to visualize these processes neurons must be transfected very sparsely. Through extensive comparison of available methods we determined that electroporation, just prior to plating, is the optimal means to achieve consistently sparsely transfected neurons (Viesselmann et al., 2011). Thus, plasmid DNA must be tolerated for up to three weeks prior to imaging while neurons mature. On the whole, wild type (WT) fluorescent constructs are relatively benign during this period of development, provided their expression is limited to the bare minimum necessary for visualization.

However, loss- or gain-of-function experiments are also critical for investigating the roles of proteins in complex biological processes like learning and memory. Even simple dominant-negative experiments can be highly informative. For example, by saturating a system with a protein fragment one can extrapolate its purpose from what goes awry. One confounding issue is that proteins involved in early development, such as axon outgrowth, dendritic branching and spinogenesis, often have conserved functions in mature neurons, for example, in

synaptic plasticity. Drebrin exemplifies such a protein, as a developmentally-regulated actin-modifying protein with diverse binding partners (Ishikawa et al., 1994; Sasaki et al., 1996; Grintsevich et al., 2014; Aoki and Sherpa, 2017). In early development drebrin facilitates neuritogenesis (Geraldo et al., 2008), axon collateral branch initiation (Ketschek et al., 2016), and generation of new dendritic spines (Yamazaki et al., 2014). Later, in mature neurons, drebrin promotes microtubule (MT) based direct-deposit of critical postsynaptic components (Merriam et al., 2013, McVicker et al., 2016), such as NMDA receptor subunits (Aoki et al., 2009; Chen at al., 2017) and PSD-95 (Mizui et al., 2005), and even aids in the postsynaptic organization of those components (Shiraishi-Yamaguchi et al., 2009). Conveniently, inducible promoters, such as tetracycline-responsive (tet-ON) systems, make it simple to delay expression of dominant-negative constructs to avoid developmental aberrations which otherwise make functional comparisons in mature neurons unfeasible.

In contrast, the complementary experiment of analyzing targeted mutations within an otherwise intact protein is an endeavor demanding greater logistic consideration. Where previously, endogenous protein was of no concern, now it's contributions represent a major confounding factor. Wholly-functional WT protein may obfuscate effects of experimental manipulations, becoming even more troublesome when proteins of interest form dimers or multimers. It may also lead to over- or misinterpretation of data, as various conflicting or complementary functions of that protein may be upregulated. Therefore, not only should mutant gene expression be delayed, but should coincide with silencing of its endogenous counterpart, such that it is replaced, rather than coexpressed. Even in a depleted background, overexpression of experimental constructs can lead to unpredictable outcomes for the very same reasons. In total, the ideal experiment would induce physiologically-matched replacement at desired time-points. Even so, no streamlined methodology has been described previously.

We recognized that currently available tools are heavily limited in their application to neuroscience and set out to develop an elegant, self-contained platform to achieve this. To do so, we sought to emulate and incorporate naturally occurring regulatory elements commonly found in the 5’ and 3’ untranslated regions (UTRs) of mammalian genes. These are diverse regions of DNA that are almost universally overlooked in the design of expression systems, but which, in cooperation with mRNA interacting elements, directly regulate mRNA stability, translation efficiency, nuclear export, localization, and ultimately control how much protein is translated (Matoulkova et al., 2012). Here we report the effective use of these materials in replacing endogenous genes with fluorescent and optogenetic constructs, and describe advantageous features of this approach which may facilitate future translation of basic research directly to therapeutics.

Materials and Methods

Plasmid Construction.

The pmAtt (miRNA / Attenuator) plasmid was constructed using the ampicillin promoter, ampicillin resistance gene, SV40 polyadenylation sequence, SV40 origin of replication, SV40 promoter, CAP binding site, lac promoter, lac operator, and beta-globin polyadenylation sequence from the widely used pCAGGS expression vector (Niwa et al., 1993). Standard molecular cloning practices including DNA digestion by restriction enzyme, DNA ligation, gene splicing by overlap extension and isothermal assembly were used to join the following sequences, in order from 5' to 3': tet-inducible promoter, Attenuator Sequence, Multiple Cloning Site comprised of AatII, SbfI, NheI, SalI, and NotI recognition sequences, mScarlet-I, EMCV IRES, variable fluorescent reporter proteins including pmiRFP670 and pmTurquoise2, enhanced mIR30 cassette, human PGK promoter, and reverse tetracycline transactivator. The resulting product was joined with the above-mentioned pCAX-sourced elements for bacterial expression and replication to complete the pmAtt gene knockdown-rescue vector. Sequences were confirmed via a Sanger sequencing service (QuintaraBio). Complete sequence maps including oligonucleotide primers used to generate gene fragments for plasmid construction are mapped digitally and available on reasonable request.

DNA Sources.

Many sources of DNA were custom-synthesized by IDT. However, commercial suppliers will not produce GC-rich sequences or those with complex secondary structures, as with an IRES or miR30 cassette. In these instances, DNA was assembled from oligonucleotide fragments via overlap extension or obtained from Addgene plasmid repository. The following major elements were acquired from:

a.) tet-inducible promoter was sourced from Addgene plasmid #41393, a gift from David Root

b.) Attenuator hairpins (Babendure et al., 2002) and Multiple Cloning Sites were ordered as oligonucleotide fragments from IDT

c.) mScarlet-I was ordered from IDT as a codon-optimized gene block based on reference Addgene plasmid #79987 (Bindels et al., 2017)

d.) EMCV IRES was sourced from Addgene Plasmid #27296, a gift from Morris Birnbaum

e.) Fluorescent reporter protein pmiRFP670 (Shcherbakova et al., 2013) was ordered from IDT as a codon-optimized gene block

f.) miR30 cassette was sourced from Addgene plasmid #73576 (Vo et al., 2016)

g.) Human PGK promoter was sourced from Addgene plasmid #41393, a gift from David Root

h.) Reverse tetracycline transactivator was sourced from Addgene plasmid #41393, a gift from David Root

i.) miRNA target sequences were ordered from IDT as ultramers

k.) MARCKS (M40) double-palmitoylated mutant membrane-anchoring domain tag was assembled via overlap extension from oligonucleotide fragments (IDT) (Karel Svoboda, Unpublished Addgene plasmid #18695)

j.) Photosensitive degradation tag (Usherenko et al., 2014) was ordered from IDT as a codon-optimized gene block

miRNA Design.

Target sites for RNA interference were chosen using the Cold Spring Harbor RNAi utility (http://katahdin.cshl.org/siRNA/RNAi.cgi?type=shRNA). Targets in the 3' UTR were given preference to avoid necessity of silent rescue gene mutation to render them insensitive.

miRNA-coding 97 nucleotide ultramers were ordered from IDT, amplified by PCR and cloned into the miR30 cassette by restriction digest with XhoI and EcoRI, and subsequent ligation.

The drebrin 97-mer sequences are as follows:

rat dbn.2310

5’-TGCTGTTGACAGTGAGCGCAAAGTTGATAGACTTGTACAATAGTGAAGCCACAGATGTAT

TGTACAAGTCTATCAACTTTTTGCCTACTGCCTCGGA-3'

rat dbn.2391

5'-TGCTGTTGACAGTGAGCGACCCAGACCAGATTGTAGCTTATAGTGAAGCCACAGATGTA

TAAGCTACAATCTGGTCTGGGCTGCCTACTGCCTCGGA-3'

The EB3 97-mer sequences are as follows:

rat mapre3.1293

5’-TGCTGTTGACAGTGAGCGCTTTGACAAAGTCATTGGTATATAGTGAAGCCACAGATGTAT

ATACCAATGACTTTGTCAAATTGCCTACTGCCTCGGA-3'

rat mapre3.1430

5’-TGCTGTTGACAGTGAGCGAACTCACCAATTCTTATTTATTTAGTGAAGCCACAGATGTAA

ATAAATAAGAATTGGTGAGTCTGCCTACTGCCTCGGA-3'

Mammalian non-targeting control 97-mer sequence based on C. elegans target MIMAT0000039 is as follows:

5'-TGCTGTTGACAGTGAGCGcACTCTTTCTAGGAGGTTGTGATAGTGAAGCCACAGATGTAT

CACAACCTCCTAGAAAGAGTATGCCTACTGCCTCGGA-3'

Rescue Gene Attenuation.

Hairpin sequences were based on previously published work (Babendure et al., 2006). RNA secondary structures and thermal stability were validated using the RNAComposer utility (Popenda et al., 2012). DNA was ordered from IDT, amplified by PCR and cloned into first position in the multiple cloning site (MCS) by restriction digest with AatII and SbfI, and subsequent ligation. The -40 kcal/mol "attenuator" was ordered as a single-stranded IDT ultramer. The ultramer (1nM) was amplified via PCR with end primers to add AatII and SbfI restriction sites. The product was directly purified using NEB Monarch PCR cleanup kit, digested, and heat inactivated. This PCR product was subcloned immediately upstream of the MCS in respective sites by adding 1ul of PCR product to 25ng cut and gel-purified vector.

-40 kcal/mol attenuator sequence is as follows:

5'-GTCAGACCGATTGATCCGGCAACAACAAGCGGTCCACCACGGCCGATATCACGGCCGT
GGTGGACCGCAACAACAACAACAACCTGCAGGCGTGTCA-3'

Amplification primers are as follows:

Forward 5'-TCATGACGTCAGACCGATTGATCCG

Reverse 5'-TGACACGCCTGCAGGTTG

Mutagenesis.

Gene modification (both mutations and generation of WT isoforms) was carried out by whole-plasmid PCR mutagenesis. Briefly, primers were designed with 18-22 nucleotides (NT) complementary to the plasmid on the 3' side and 8-10 NT complementary 5' sequences. The 5' complement flanked the desired DNA insertion or substitution, or for deletions, simply omitted

the NT present in the template. A reaction containing 25uL Q5 2x master mix (NEB), 10ng template plasmid, and 2.5uM forward and reverse primers was diluted with PCR grade water up to 50uL. This reaction was pipetted gently to mix, touch-centrifuged and thermocycled according to specifications for Q5 polymerase. Mutagenized plasmid DNA was purified with Monarch PCR Cleanup kit (NEB), then treated for 30 minutes with 1uL DpnI in CutSmart buffer to digest methylated template DNA. DpnI was heat-inactivated at 80°C following digestion and 5ul was immediately transformed into chemically competent bacteria (E.Cloni, Lucigen) following manufacturer guidelines. Results were confirmed by Sanger sequencing (QuintaraBio).

Cell Culture and Transfections.

Primary hippocampal neurons were prepared from Sprague Dawley rats (Harlan) at E18.5 (McVicker et al., 2016). Briefly, rat hippocampi were dissected, trypsinized and transfected with plasmid DNA while in suspension using the Lonza Nucleofector, per manufacturer instructions. Neurons were plated at a density of $3x10^4$ neurons per cm^2 on 1 μg/ml PEI (Sigma)-coated coverslips, which were adhered to 35 mm plastic culture dishes containing a 15 mm hole drilled through the chamber. Neurons were plated with plating media (PM; neurobasal media with 5% fetal bovine serum (FBS), B27 supplement, 2 mM glutamine, 0.3% glucose and 37.5 mM NaCl) for 1 h at 5.0% CO_2 and 37°C, after which the chambers were flooded with 2 ml of serum-free media (PM with no added FBS). For tet-ON promoter induction 1μg/μL doxycycline was maintained in culture media for 7 days prior to imaging. All procedures were approved by the University of Wisconsin Committee on Animal Care and were in accordance with the NIH guidelines.

Immunocytochemistry, Image Acquisition, Processing and Analysis.

Neurons were fixed in 4% paraformaldehyde-Krebs buffer-sucrose at 37°C (Dent and Meiri, 1992), rinsed in PBS, blocked with 10% BSA and permeabilized in 0.2% Triton X-100. Neurons were incubated for 1 h at room temperature with primary rabbit anti-Drebrin antibody (1:500 Abcam ab60933), followed by a 1 h incubation with secondary goat anti-rabbit alexa-568-conjugated antibodies (1:500; Life Technologies). Image stacks of fixed neurons were acquired using a 63x/1.4NA objective on a Zeiss LSM800 scanning confocal microscope. Comparison images of controls, miRNA expressing neurons and knockdown/rescue neurons were created in Fiji (Schindelin et al., 2012).

Western Blotting and Protein Analysis.

Rat cortical cultures were lysed at DIV 9 in NP40 buffer with antiprotease and antiphosphatase tablets (Roche). Protein was quantified with the bicininchronic acid (BCA) colorimetric assay (Pierce) and diluted with dithiothreitol (reducing agent) and LDS sample buffer (NuPage). The samples were heated at 95°C for 5 minutes, vortexed and cooled on ice. Samples (40µg/well) were loaded and transferred onto PVDF membranes for 1 hour at 90V on ice. Membranes were blocked with non-fat dry milk (5%) for 1 hour and incubated with primary antibody (Rabbit anti-EB3, ABCAM 1:200; Rabbit anti-drebrin ABCAM 1:200) overnight at 4°C. Membranes were then rinsed 3x with TBS-T and incubated with HRP-Protein A (Invitrogen 1:1000) for one hour. The Pierce ECL Plus Western Blotting Substrate Kit (Thermo Scientific) was used according to manufacturer's protocol. Band were visualized with a UVP ChemiDocIt system and analyzed with VisionWorks image acquisition and analysis software.

Results

Conception, construction and validation of inducible system for gene silencing and rescue

Our primary goal was to establish a single-plasmid solution for reliable, temporally linked depletion of endogenous protein with concomitant rescue expression. The ideal system would, within one otherwise identical backbone, permit direct comparison between overexpressed, silenced, and both WT and mutant rescue conditions for any chosen protein. Whether through endogenous cellular mechanisms or researcher-introduced, RNA interference (RNAi) ultimately requires generation of small, single-stranded DNA fragments which bind target transcripts by base-recognition and subsequently recruit the RNA-induced silencing complex (RISC), which eliminates it (Hammond 2000). Popular approaches to achieve gene silencing via RNAi have a range of limitations. For example, synthetic small interfering RNA (siRNA) are potent activators of the mammalian innate immune response and are only transiently effective (Judge et al., 2008). Alternatively, long-term and inducible suppression of target genes can be accomplished with available siRNA/miRNA vectors, but these require specific pol III, typically U6 or H1, promoters to function. Their incorporation therefore requires co-expression of various plasmids, or expansion of a single plasmid with additional promoters, both of which undermine potential clinical value. However, miRNA biogenesis provides an attractive alternative. Researchers have demonstrated that native miRNA cassettes vastly outperform the silencing potency of traditional vectors on a per-copy basis, lowering potential antigenic responses as well (Fellmann et al., 2013). The expression of most human protein coding genes is naturally regulated by at least 1,000 different miRNAs (Lewis et al., 2005; Friedman et al., 2009). Many miRNAs reside within introns and even exons of genes, frequently co-localize in regulatory clusters, and may even be found on transcripts coding proteins they will later target (Rodriguez et al., 2004; Vidigal and Ventura 2015). We reasoned this could be emulated to great effect in an artificial construct.

In total, our original plasmid design **(Fig. 1)** employs a current generation, tight doxycycline-inducible (tet-ON) promoter with its corresponding transactivator (rTTA) gene downstream of a PGK promoter, which drives constitutive and uniform expression across many cell types (Chen et al., 2011). This permits us to delay expression of our construct by withholding doxycycline until neuronal maturity. To temporally lock endogenous gene silencing and replacement a single-transcript approach incorporates an intact mir30 cassette in the 3' UTR of our rescue gene. Advantageously, this system will function downstream of any pol II or III promoter (Fellmann et al., 2013). For visual identification of induced cells, we included a fluorescent cell membrane label and tandem 2A peptide cleavage sequences from porcine teschovirus-1 polyprotein (P2A) and thosea asigna virus 2A (T2A) flanking the rescue gene on its 5' side. This achieves complete separation by ribosome-skipping in the formation of a glycyl-prolyl peptide bond at both 2A C-termini (Liu et al., 2017).

We chose to validate this strategy using the actin-associated protein drebrin, which functions both in early developmental processes like neuritogenesis and axon guidance, and later postsynaptic processes (Chen at al., 2017). First, we evaluated two RNAi targets located in the drebrin 3' UTR, one beginning at nucleotide 2310 and the second at 2391. Preferentially targeting untranslated regions which are not included in the construct itself simplifies rescue expression by avoiding otherwise requisite silent mutations to render the rescue gene insusceptible to silencing. Rat cortical neurons were transfected on the day of plating and permitted to mature undisturbed for 14 days before a 7 day induction of the knockdown and rescue. We found that both 3' UTR targets were effective independently, and modestly more potent when co-transfected **(Fig. 2)**. However, due to incomplete transfection efficiency of nucleofection (we average ~50% of neurons) we cannot accurately estimate the percentage reduction in drebrin.

To evaluate drebrin reduction further on a cell-by-cell basis, primary hippocampal cultures were prepared in two conditions. First, plasmid DNA was transfected encoding the RFP membrane label reporter and drebrin targeting miRNA to confirm RNAi efficacy and drebrin depletion by immunocytochemistry (ICC) **(Fig. 3**, top row**)**. In the second condition, we transfected the identical construct plus the drebrin-GFP rescue gene inserted to visually confirm rescue **(Fig. 3**, bottom row**)**. When drebrin-GFP is over-expressed during development, it later contributes to actin accumulation and elongation of dendritic spines into what have been termed "megapodia" (Mizui et al., 2005). We see no such morphological phenotype when we silence endogenous drebrin expression in adult neurons and rescue with WT drebrin-GFP, suggesting total levels remain within a physiologically relevant range. Thus, in this design iteration we demonstrate inducible, temporally-locked depletion and rescue expression of target proteins in neurons.

Design revisions to improve flexibility of rescue expression level

Though drebrin rescue expression clearly did not cause commonly observed drebrin overexpression artifacts, additional validation by Western blot analysis of neuronal lysate revealed that drebrin-GFP rescue expression was indeed at greater levels than endogenous expression (data not shown). This expression could theoretically be matched to endogenous levels by titrating doxycycline induction, but this method would be problematic for several reasons. Doxycycline is stable at 4^{o}C, but has a half-life in media of 48 hours, thus requiring frequent replacement to maintain an effective concentration. Therefore, attempting to maintain protein expression at consistent, but less-than-maximal, induction over time is impractical. Drebrin, for example, would represent a particularly challenging target with this strategy because of an extraordinarily stable synaptic half-life of 6.23 days (Cohen et al 2013).

Furthermore, our knockdown-rescue (KDR) plasmid was intentionally designed with a feed-forward loop to produce additional transactivator following induction, so titration could not be accomplished in a linear fashion. The necessity of a single transcript to link rescue protein expression, miRNA delivery and reporter fluorescence raises a still-larger predicament. Lowering promoter induction and total mRNA level to match endogenous protein expression would be at the cost of reporter brightness and silencing potency. Considering this, it was logical that manipulating translation, rather than transcription, represented our best avenue forward.

Traditionally, primary regulation of gene expression is considered to occur at the level of transcription, where base promoter strength, modified in major capacity by recruitment of activation and other promoter elements, dictates final expression levels (Matoulkova et al., 2012). Promoter strength is also the primary determinant in nearly all conventional expression systems. However, we are continually broadening our understanding of how 5' UTR mRNA structures regulate translation. The high GC content typical of 5’ UTRs naturally predisposes mRNA transcripts to secondary structure formation. These range from simple hairpin loops, to elaborate, highly structured elements like internal ribosome entry sites (IRESs) (Leppek et al., 2018). Some even require binding of additional permissive factors for standard preinitiation complex formation and subsequent translation to occur at all (Pisareva 2008). We reasoned that a hard-coded, tuneable “brake” at the mRNA level could be implemented to control translation. After extensive review and consideration of attenuation strategies, manipulating thermal stability hairpin structures between the 5’ cap and initiation codon of our rescue gene emerged as the best option. Such elements have been described to exhibit an inverse relationship between the thermal stability of RNA secondary structure and translation efficiency (Babendure et al., 2002), likely by hindrance of pre-initiation complex recognition and assembly (Luse 2014). Beyond dictating translation efficiency, addition of this feature would also improve core functionality of

our platform in two major ways: First, by enhancing the consistency of expression by permitting uniformly maximal promoter induction and Second, as a consequence of maximal promoter induction and greater total transcript number, we proportionally increase gene silencing potency.

When hairpin stability is -40 kcal/mol or greater, translation efficiency is determined by a relatively complex relationship between the distance of the loop to both the 5' cap of the transcript and the gene's start codon. However, at higher stability this positioning ceases to have any significant impact and further increase exhibits steeply diminishing return (Babendure et al., 2002). Therefore, to maximize both the predictability and intensity of rescue gene attenuation, we chose to perform our initial test of this strategy with an "attenuator" sequence of -40 kcal/mol. This attenuator sequence was synthesized and cloned between the tet-ON promoter and rescue gene multiple cloning site (MCS), such that translation of any rescue gene cloned into the first MCS position should be attenuated uniformly. To determine the effectiveness of this approach we chose to silence the microtubule (MT) plus end tracking protein EB3 and rescue with EB3-RFP. Four EB3-RFP expressing plasmids were compared. Two conditions featured non-targeting miRNA, one of which with a rescue gene attenuator (-40/miRNA X) and one without (0/miRNA X) to compare attenuation directly. Two additional plasmids featured miRNA targeting the rat EB3 3' UTR (-40/miRNA 1 and -40/miRNA 2) to determine the proportion of EB3 silenced versus EB3-RFP expressed.

As before, rat cortical neurons were transfected, plated, and allowed to mature for 14 days before induction with doxycycline for 7 days, and collection of lysate for Western blot analysis. EB3 has a molecular weight of 32 kDa, whereas RFP (mScarlet) is 25 kDa. As such, rescue expression of EB3-RFP appears as a distinct band just under twice the size of endogenous EB3, facilitating easy comparison **(Fig. 4)**. Relative to endogenous levels, normal expression of EB3, downstream of the tet-ON promoter, was nearly three-fold higher (298%). In

stark contrast, attenuated mRNA yielded only 57% endogenous expression levels, six-fold less EB3-RFP than the unmodified transcript. Endogenous EB3 was reduced 45% by miRNA 1, and 40% by miRNA 2. Unexpectedly, we also observed a third band above EB3-RFP. In separate control experiments no doublet is observed for endogenous EB3 alone. This band is consistent between replicate experiments and is presumed to be the result of post-translational modification, likely ubiquitination, specific to this EB3-RFP construct. As with earlier quantification of drebrin silencing by Western blot **(Fig. 2)**, due to sparse transfection these measures are under-estimates of knockdown and replacement within individual neurons, in all conditions. In total, these experiments clearly demonstrate that our revised plasmid design selectively attenuates rescue gene translation, and while not rigorously quantitative, we estimate that roughly as much endogenous EB3 is being eliminated as EB3-RFP is being expressed in its stead.

Insulating fluorescent reporter from attenuation to maintain brightness

With our validation that mRNA-encoded attenuators reduce rescue gene translation as anticipated, we set upon addressing a key pitfall of this new design. While originally a critical design element, our membrane reporter scheme relied on 2A peptide cleavage to be produced as a separate protein by-product of our rescue gene. A single start codon is shared between both rescue and reporter cistrons **(Fig. 4)**. Therefore, because the attenuator reduces rescue protein translation by impeding its initiation, a decidedly unwanted consequence is the proportional reduction in reporter brightness. It is worth noting that it would not be unreasonable to instead conjoin the reporter and transactivator downstream of the hPGK promoter. Transfected cells would still be easily identified, however, we would lose the original functionality provided by a reporter tied to induction itself, which indicates targeted gene

replacement. Granted, targeted gene replacement could also be confirmed by direct tagging of the rescue product, but this is not always possible. Instead, to preserve this functionality we sought ways to maintain single-transcript design, but prevent reporter attenuation. Eukaryotic 5′ UTRs may contain an internal ribosome entry sites (IRES), which is a cap-independent method of translational activation. An IRES allows for direct binding of the ribosomal complexes to the transcript to begin translation, eliminating the need for a pre-initiation complex at the 5′ cap (Brown, 2007). While this feature was originally borne of viral necessity for quick replication, we reasoned this could be employed effectively to insulate our reporter by providing an independent start site in the middle of our mRNA transcript.

However, the efficacy of IRES elements in expression systems is a historical point of contention, and root of serious reproducibility issues (Bochkov et al., 2006). Variability in reported outcomes from publicly available plasmids can be traced back at least in part to their origins as commercial vectors. For example, the popular Picornaviridae family encephalomyocarditis virus (EMCV) IRES which was first isolated in 1945 (Carocci and Bakkali-Kassimhas 2012) has since been subjected to miscellaneous iterative modifications by various hands, with the goal of increasing its ease of use in cloning applications. Because these truncations and substitutions reduced its efficacy, an anecdotal rule states the IRES 3’ cistron will always suffer low yield compared to its 5’ cistron. To the contrary, in its native conformation the EMCV IRES may achieve equivalent or greater translation than cap-dependent initiation (Bochkov et al., 2006). Considering this, we reversed positions of the rescue gene and reporter, and replaced the original 2A site with a complete EMCV IRES **(Fig. 5)**. Assembly was performed seamlessly by overlap extension splicing to ensure ideal M-loop positioning and maximal reporter production. Two primary variants were created, with either IRES-mediated far-red (pmiRFP670, Shcherbakova et al., 2013) or blue (mTurquoise2, Goedhart et al., 2012)

membrane-label reporters, and an upstream multiple cloning site to insert rescue constructs with a red (mScarlet-i) fusion tag **(Fig. 5 and Supplemental Fig. 1)**.

Protein replacement with photo-degradable variants and focal elimination in neurons

Similar to our endeavors studying targeted mutations in neurons, a generally recognized issue in optogenetics is that heterogeneity in expression of experimental constructs and wild-type protein causes issues with reliability and reproducibility (Kramer et al., 2013). Many optogenetic constructs employ Light-Oxygen-Voltage (LOV) domains, light-responsive proteins found in a large variety of plants, algae, fungi and bacteria (Pudasaini et al., 2015). LOV domains consist of a flavin mononucleotide-binding core domain and Jα-helical extension at the carboxy-terminus **(Fig. 6B)**. Light induces conformational change within the core, followed by unfolding of the Jα helix, which reveals an otherwise cryptic kinase domain, and catalyzes a variety of signaling cascades depending on the specific organism (Pudasaini et al., 2015). Recent chimeric substitution of the ornithine decarboxylase (ODC) proteasomal recognition sequence in place of the LOV kinase domain allows for rapid degradation of proteins of interest. ODC is an extraordinarily short-lived enzyme with a half life of only 30 minutes, a characteristic owed to rapid ubiquitin-independent degradation mechanisms (Usherenko et al., 2014), which is imparted to the proteins tagged with this photo-sensitive degron (PSD), when exposed to blue light. One may thus achieve rapid, specific elimination of PSD-tagged proteins.

Despite this utility, unless one addresses background expression the best such experiments can achieve are observations of overexpression, followed by a return to baseline after degradation. Thus, we saw this as an excellent opportunity to use our KDR platform. Because of the natural absorption spectrum of LOV domains this technique reserves wavelengths shorter than 488 nm for activation. We are therefore restricted to RFP and longer

wavelength proteins for fluorescence imaging. To account for this limitation we cloned a far-red (pmiRFP670, Shcherbakova et al., 2013) reporter into the KDR vector. Two PSD-tagging variants were made subsequently. First, a RFP-PSD tag to visually confirm target degradation **(Fig 6A)**, and second, an otherwise identical but non-fluorescent PSD tag to cover applications where direct visualization may not be necessary or possible (not shown). To test whether this technique could be used to focally degrade proteins of interest in mature neurons we subcloned our previously validated drebrin KDR miRNA sequence and WT drebrin into to the RFP-PSD tagging plasmid. Hippocampal neurons were transfected with this plasmid, allowed to mature and induced as earlier described to replace endogenous drebrin with drebrin-RFP-PSD. Single dendritic branches were scanned with 0.20% power 488 nm light at 1 μsec pixel dwell time, in between acquisitions of drebrin-RFP-PSD signal. Drebrin fluorescence was reliably diminished relative to adjacent dendrites **(Fig. 6C)**. This decrease in protein concentration occurred over the expected time-course and with the application of less intense blue light than used in routine imaging. This experiment further demonstrates the value and versatility of this platform, not only to study mutations, but also for uniformly tagging or otherwise modifying all of a chosen protein within a cell.

Discussion

Currently available tools for examining the effects of targeted mutations are heavily limited in their application to neuroscience. A streamlined knockdown-replacement strategy to study protein function has not previously been described in any methodical way. Thus, we set out to develop a self-contained, versatile platform for genetic manipulation. After considerable research, testing, and revision of approach and materials we produced a novel plasmid toolkit for inducible, reversible gene silencing and replacement. We achieved this knockdown-rescue (KDR) by combining heavily engineered staples of modern expression systems with natural regulatory elements of mammalian untranslated regions (UTR), which are vastly overlooked in most expression systems. With this construct we demonstrate physiologically-tunable replacement of endogenous proteins with “rescue” constructs. This strategy may be applied in a variety of experimental paradigms. For example, for simple visualization of target proteins with fluorescent tags, replacement of endogenous protein with functional mutants, or application of more complex tags to modify protein behavior. In Chapter 2 we applied this technique to evaluate EB3-drebrin interaction in mature neurons with mutant constructs targeting putative binding domains. Also, as a proof-of-principle experiment we used this construct to focally manipulate the stability of drebrin in mature neurons by turnover with a chimeric, photo-sensitive degron (PSD) tagged version (Usherenko et al., 2014). Though drebrin naturally has a synaptic half-life of over six days (Cohen et al., 2013), we were able to focally deplete drebrin-RFP-PSD from dendritic spines in mature cultured hippocampal neurons in under an hour, with spatially restricted application of 488 nm light. This proof-of-concept experiment illustrates high potential for delivery and usage of other optogenetic probes, including ion channels and light controlled dimers, which currently suffer many of the same methodological pitfalls as mentioned above. We expect that by reducing the necessity of direct chromosomal editing (i.e. with CRISPR/Cas9

technology) to employ these techniques (Usherenko et al., 2014), this KDR platform will dramatically increase the practical accessibility of the PSD and other tags.

We originally conceived of this technique as a means of replacing endogenous proteins with functional mutants; a means of perturbing healthy cells to understand the effects of targeted mutations. However, the reverse is also equally feasible. In the case of diseases with genetic etiology, and with a proper therapeutic vector to administer it, this approach could be applied as a genetically engineered strategy to replace mutant with functional proteins. The first AAV gene therapy is only now being approved by the FDA (Smalley 2017). While this is a monumental step forward, options are, and will likely remain, limited for quite some time. Innate immunity poses great challenges to effective gene therapy, and most diseases of the CNS would require systemic administration of vectors (Basner-Tschakarjan and Mingozzi, 2014). As such, second chances will be practically unheard of. In the clinical realm, and with advancement toward personalized medicine, a pre-verified, portable therapeutic agent would be hugely useful. As designed, this single-transcript approach is entirely vector agnostic **(Supplemental Fig. 2)**. Though tools used in primary research are seldom directly translatable to clinical application, this portability means that any therapeutic strategy verified *in vitro* could be transferred easily to gene-therapy vectors, and seamlessly benefit from future advances in their delivery.

References

Aoki C, Kojima N, Sabaliauskas N, et al. Drebrin a knockout eliminates the rapid form of homeostatic synaptic plasticity at excitatory synapses of intact adult cerebral cortex. J Comp Neurol. 2009;517(1):105-21.

Aoki C, Sherpa AD. Making of a Synapse: Recurrent Roles of Drebrin A at Excitatory Synapses Throughout Life. Adv Exp Med Biol. 2017;1006:119-139.

Babendure JR, Babendure JL, Ding JH, Tsien RY. Control of mammalian translation by mRNA structure near caps. RNA. 2006;12(5):851-61.

Bochkov YA, Palmenberg AC. Translational efficiency of EMCV IRES in bicistronic vectors is dependent upon IRES sequence and gene location. BioTechniques. 2006;41(3):283-4, 286, 288 passim.

Chen YW, Actor-engel H, Sherpa AD, Klingensmith L, Chowdhury TG, Aoki C. NR2A- and NR2B-NMDA receptors and drebrin within postsynaptic spines of the hippocampus correlate with hunger-evoked exercise. Brain Struct Funct. 2017;222(5):2271-2294.

Cohen LD, Zuchman R, Sorokina O, et al. Metabolic turnover of synaptic proteins: kinetics, interdependencies and implications for synaptic maintenance. PLoS ONE. 2013;8(5):e63191.

Fellmann C, Hoffmann T, Sridhar V, et al. An optimized microRNA backbone for effective single-copy RNAi. Cell Rep. 2013;5(6):1704-13.

Fellmann C, Hoffmann T, Sridhar V, et al. An optimized microRNA backbone for effective single-copy RNAi. Cell Rep. 2013;5(6):1704-13.

Friedman RC, Farh KK, Burge CB, Bartel DP. Most mammalian mRNAs are conserved targets of microRNAs. Genome Res. 2009;19(1):92-105.

Geraldo S, Khanzada UK, Parsons M, Chilton JK, Gordon-weeks PR. Targeting of the F-actin-binding protein drebrin by the microtubule plus-tip protein EB3 is required for neuritogenesis. Nat Cell Biol. 2008;10(10):1181-9.

Grintsevich EE, Reisler E. Drebrin inhibits cofilin-induced severing of F-actin. Cytoskeleton (Hoboken). 2014;71(8):472-83.

Ishikawa R, Hayashi K, Shirao T, et al. Drebrin, a development-associated brain protein from rat embryo, causes the dissociation of tropomyosin from actin filaments. J Biol Chem. 1994;269(47):29928-33.

Judge A, Maclachlan I. Overcoming the innate immune response to small interfering RNA. Hum Gene Ther. 2008;19(2):111-24.

Ketschek A, Spillane M, Dun XP, Hardy H, Chilton J, Gallo G. Drebrin coordinates the actin and microtubule cytoskeleton during the initiation of axon collateral branches. Dev Neurobiol. 2016;76(10):1092-110.

Lam RS, Töpfer FM, Wood PG, Busskamp V, Bamberg E. Functional Maturation of Human Stem Cell-Derived Neurons in Long-Term Cultures. PLoS ONE. 2017;12(1):e0169506.

Lau P, De strooper B. Dysregulated microRNAs in neurodegenerative disorders. Semin Cell Dev Biol. 2010;21(7):768-73.

Leppek K, Das R, Barna M. Functional 5' UTR mRNA structures in eukaryotic translation regulation and how to find them. Nat Rev Mol Cell Biol. 2018;19(3):158-174.

Lewis BP, Burge CB, Bartel DP. Conserved seed pairing, often flanked by adenosines, indicates that thousands of human genes are microRNA targets. Cell. 2005;120(1):15-20.

Liu Z, Chen O, Wall JBJ, et al. Systematic comparison of 2A peptides for cloning multi-genes in a polycistronic vector. Sci Rep. 2017;7(1):2193.

Luse DS. The RNA polymerase II preinitiation complex. Through what pathway is the complex assembled?. Transcription. 2014;5(1):e27050.

Matoulkova E, Michalova E, Vojtesek B, Hrstka R. The role of the 3' untranslated region in post-transcriptional regulation of protein expression in mammalian cells. RNA Biol. 2012;9(5):563-76.

Mcvicker DP, Awe AM, Richters KE, et al. Transport of a kinesin-cargo pair along microtubules into dendritic spines undergoing synaptic plasticity. Nat Commun. 2016;7:12741.

Merriam EB, Millette M, Lumbard DC, et al. Synaptic regulation of microtubule dynamics in dendritic spines by calcium, F-actin, and drebrin. J Neurosci. 2013;33(42):16471-82.

Mizui T, Takahashi H, Sekino Y, Shirao T. Overexpression of drebrin A in immature neurons induces the accumulation of F-actin and PSD-95 into dendritic filopodia, and the formation of large abnormal protrusions. Mol Cell Neurosci. 2005;30(1):149-57.

Pisareva VP, Pisarev AV, Komar AA, Hellen CU, Pestova TV. Translation initiation on mammalian mRNAs with structured 5'UTRs requires DExH-box protein DHX29. Cell. 2008;135(7):1237-50.

Rodriguez A, Griffiths-jones S, Ashurst JL, Bradley A. Identification of mammalian microRNA host genes and transcription units. Genome Res. 2004;14(10A):1902-10.

Sasaki Y, Hayashi K, Shirao T, Ishikawa R, Kohama K. Inhibition by drebrin of the actin-bundling activity of brain fascin, a protein localized in filopodia of growth cones. J Neurochem. 1996;66(3):980-8.

Schindelin J, Arganda-Carreras I, Frise E, et al. Fiji: an open-source platform for biological-image analysis. Nat Methods. 2012;9(7):676-82.

Shiraishi-Yamaguchi Y, Sato Y, Sakai R, et al. Interaction of Cupidin/Homer2 with two actin cytoskeletal regulators, Cdc42 small GTPase and Drebrin, in dendritic spines. BMC Neurosci. 2009;10:25.

Vidigal JA, Ventura A. The biological functions of miRNAs: lessons from in vivo studies. Trends Cell Biol. 2015;25(3):137-47.

Viesselmann C, Ballweg J, Lumbard D, Dent EW. Nucleofection and primary culture of embryonic mouse hippocampal and cortical neurons. J Vis Exp. 2011;(47)

Wu Z, Yang H, Colosi P. Effect of genome size on AAV vector packaging. Mol Ther. 2010;18(1):80-6.

Yamazaki H, Kojima N, Kato K, et al. Spikar, a novel drebrin-binding protein, regulates the formation and stabilization of dendritic spines. J Neurochem. 2014;128(4):507-22.

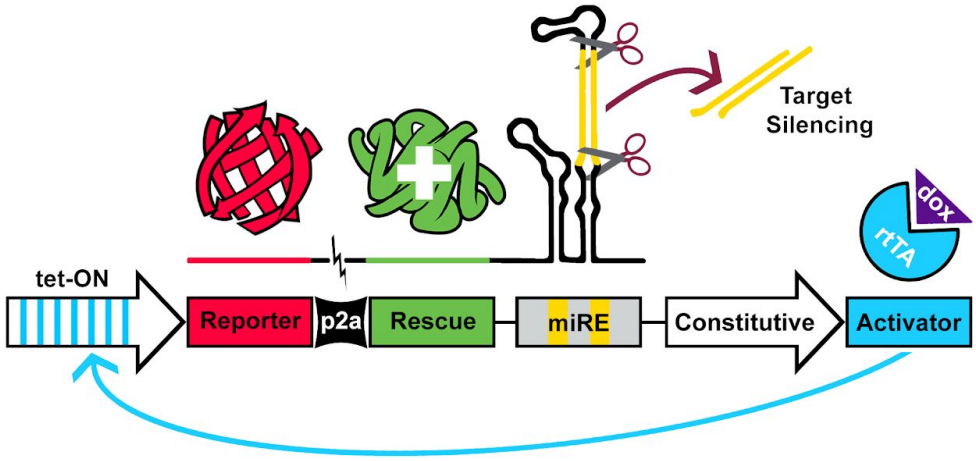

Fig. 1) Diagram of knockdown-replacement strategy.

Bottom schematic represents plasmid DNA, with resulting RNA transcript secondary structure shown above. Protein products are illustrated above corresponding coding regions. Our original tet-ON driven, single transcript design features an RFP-membrane reporter co-translated with a rescue gene as separate products via P2A cleavage. RNAi is accomplished via the 3' UTR mir30 cassette, cleaved into miRNA which targets, preferentially, noncoding regions of the endogenous gene of interest. This eliminates the need of introducing silent mutations into the rescue gene to render it insensitive to RNAi. Human PGK promoter drives constitutive and uniform transactivator (rTTA) expression across many cell types. Tet-inducible (tet-ON) promoter permits delay of expression by withholding doxycycline until knockdown-replacement is required (i.e. after neurons mature).

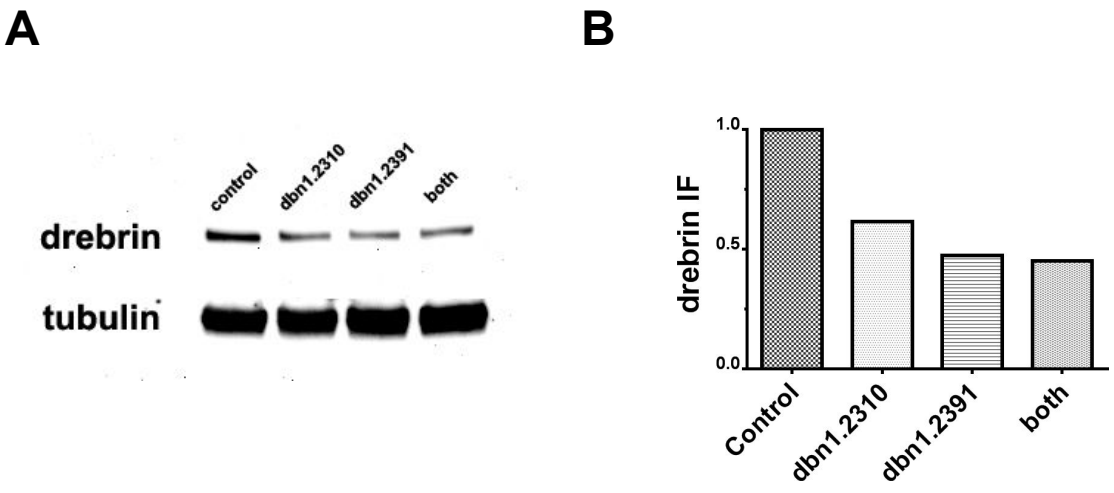

Fig. 2) Validation of drebrin silencing by targeting its 3' UTR.

(A) Rat cortical neurons were sparsely transfected (~50%) with constructs targeting different regions of the drebrin 3' UTR (dbn1.2310 and dbn1.2391) or non-targeting miRNA (control). Cells were allowed to mature for 14 DIV before 7 day induction with doxycycline and collection of lysate. Western blot analysis indicated both RNAi targets were effective in silencing endogenous drebrin expression. **(B)** Band intensity (drebrin Immunofluorescence (IF)) is graphed as a proportion of control. Given that dbn1.2391 exhibited slightly greater potency than dbn1.2391 and the addition of both miRNAs were not additive, dbn1.2391 was chosen for future applications.

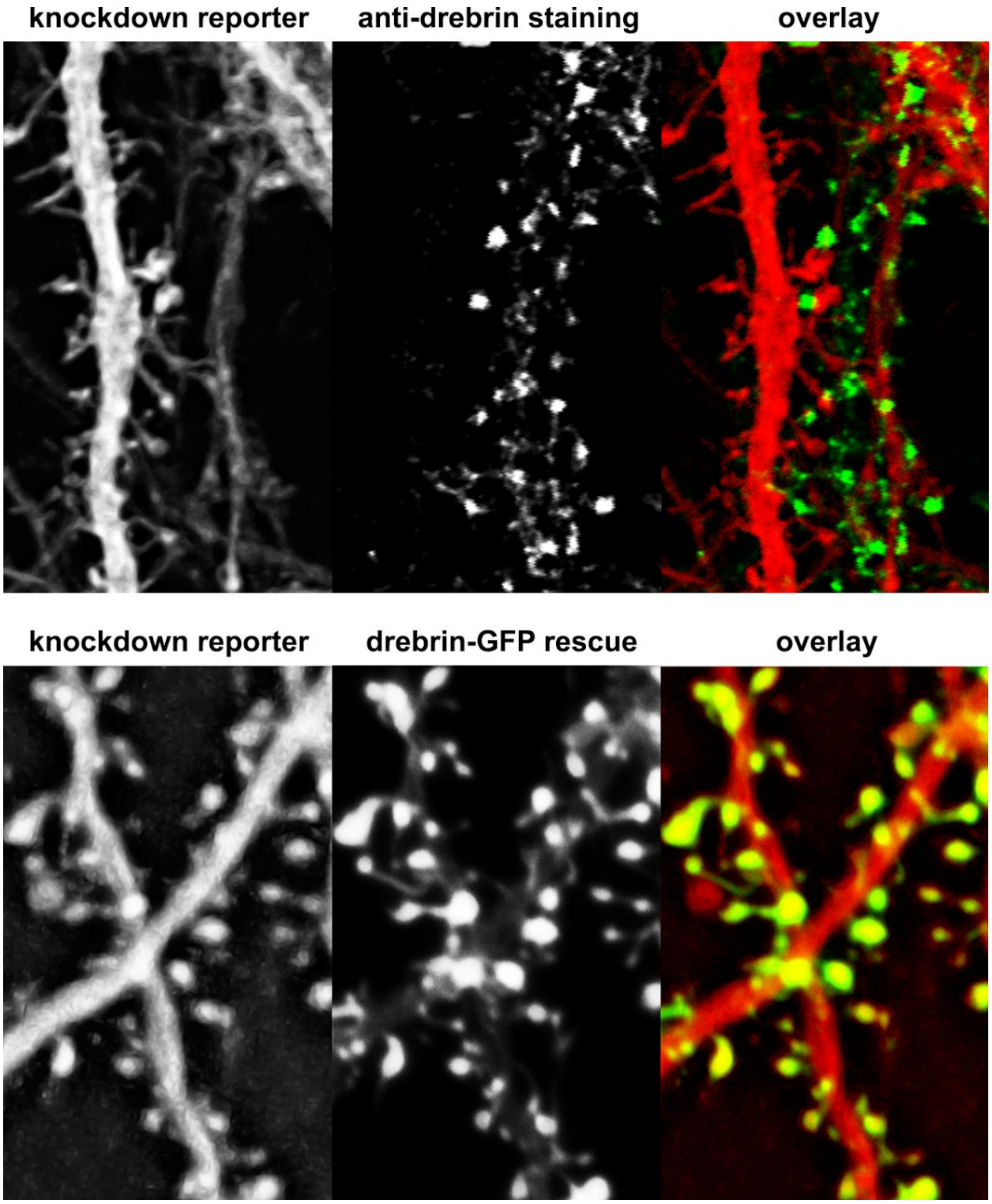
knockdown reporter
anti-drebrin staining
overlay
knockdown reporter
drebrin-GFP rescue
overlay

Fig. 3) Validation of simultaneous reporter expression and knockdown-rescue. Hippocampal cultures were sparsely transfected with plasmid encoding either drebrin-targeting miRNA and no rescue gene, or drebrin-GFP rescue gene and drebrin-targeting miRNA. Cultures were allowed to mature for 14 days prior to tet-ON promoter induction with doxycycline. Cultures were fixed at 21 days and miRNA-only dishes were immunostained with anti-drebrin antibody. miRNA reporter-expressing cells are entirely depleted of drebrin, while adjacent non-transfected cell is revealed by robust anti-drebrin fluorescence (top). The overlay confirms effectiveness of RNAi. The thin reporter-labeled process is likely an axon running parallel to an unlabeled dendrite that is labeled for drebrin. Knockdown-rescue with drebrin-GFP yields morphologically normal dendritic spines. Replacement drebrin-GFP localizes with specificity to dendritic spines, much the same as endogenous drebrin (bottom).

A

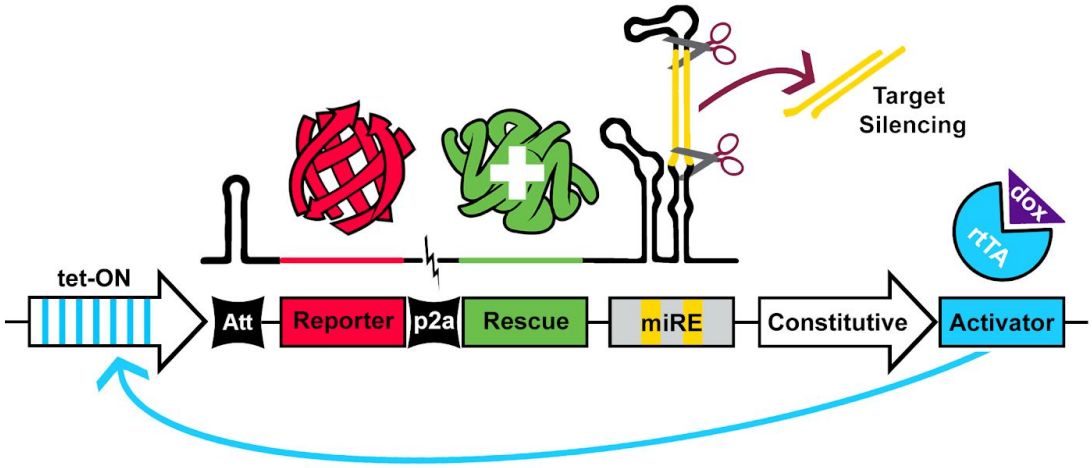
Target
Silencing
dox
rtTA
tet-ON
Att
Reporter
p2a
Rescue
miRE
Constitutive
Activator

B

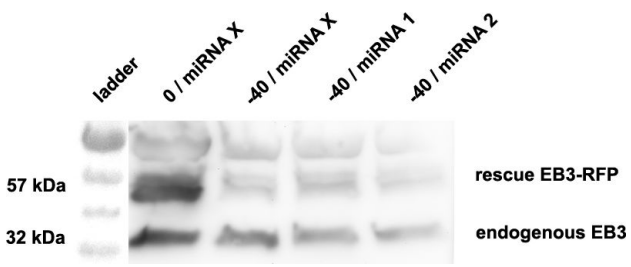
ladder
0 / miRNA X
-40 / miRNA X
-40 / miRNA 1
-40 / miRNA 2
57 kDa
32 kDa
rescue EB3-RFP
endogenous EB3

C

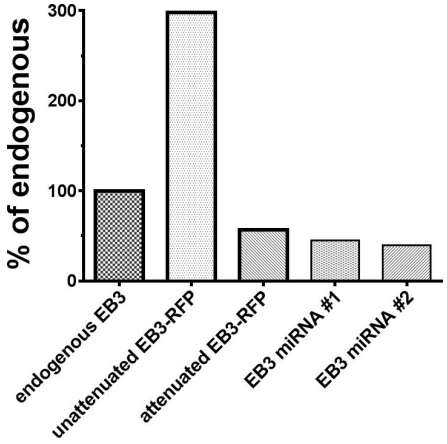
% of endogenous
300
200
100
0
endogenous EB3
unattenuated EB3-RFP
attenuated EB3-RFP
EB3 miRNA #1
EB3 miRNA #2

Fig. 4) Knockdown of endogenous EB3 and replacement with physiologically relevant levels of EB3-RFP.

(A) Diagram of vector used in this experiment. **(B)** Rat cortical neurons were transfected, plated, and allowed to mature for 14 days before induction with doxycycline for 7 days, and collection of lysate for Western blot analysis. Four EB3-RFP expressing plasmids were compared. Two conditions featured non-targeting miRNA, one without a rescue gene (0/miRNA X) and one with an attenuated rescue gene (-40/miRNA X) to compare attenuation directly. Two additional plasmids featured miRNA targeting of the rat EB3 3' UTR (-40/miRNA 1 and -40/miRNA 2) to determine the proportion of EB3 silenced versus EB3-RFP expressed. EB3 has a molecular weight of 32 kDa, whereas RFP (mScarlet) is 25 kDa, therefore rescue expression of EB3-RFP appears at 57 kDa. **(C)** Quantification of Western blot. Unattenuated expression of EB3 by the tet-ON promoter was nearly three-fold higher (298%) than endogenous levels. Attenuated mRNA yielded only 57% endogenous expression levels, six-fold less EB3-RFP than unmodified transcript. Endogenous EB3 was reduced 45% by miRNA #1, and 40% by miRNA #2. All measurements are underestimates due to sparse transfection (~50%) efficiency in neurons.

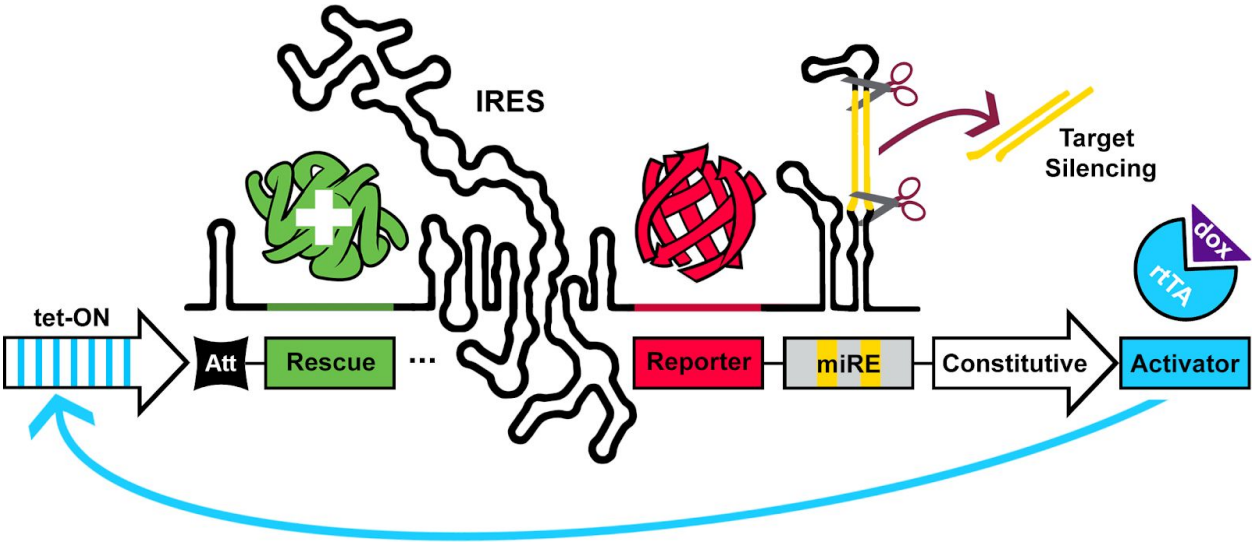

Fig. 5) Diagram of pmAtt2.0 vector for knockdown and physiological replacement. Bottom schematic represents plasmid DNA, with resulting RNA transcript secondary structure shown above. Protein products are illustrated above corresponding coding regions. Our novel design employs a current generation, tight doxycycline-inducible promoter and its corresponding transactivator (rTTA) gene downstream of a PGK promoter, which drives constitutive and uniform expression across many cell types. This permits us to delay expression of our construct by withholding doxycycline until neuronal maturity. A unique, single transcript approach incorporating a mir30 cassette in the 3' UTR of our rescue gene temporally locks endogenous gene silencing and replacement, and in contrast to most common siRNA/shRNA delivery methods, functions downstream of any Pol II or III promoter. Physiologically tunable attenuation of rescue gene translation is achieved by interchangeable 5' UTR hairpins which act as graded steric blocks to ribosomal initiation. RNAi efficiency is enhanced because total transcript production may be increased, while maintaining appropriate total levels of rescue protein. Placement of a genetically encoded fluorescent cell membrane reporter downstream of an IRES element provides a separate initiation site for translation unaffected by 5' UTR attenuator.

A

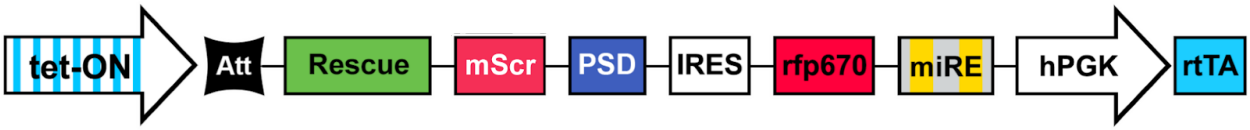
tet-ON
Att
Rescue
mScr
PSD
IRES
rfp670
miRE
hPGK
rtTA

B

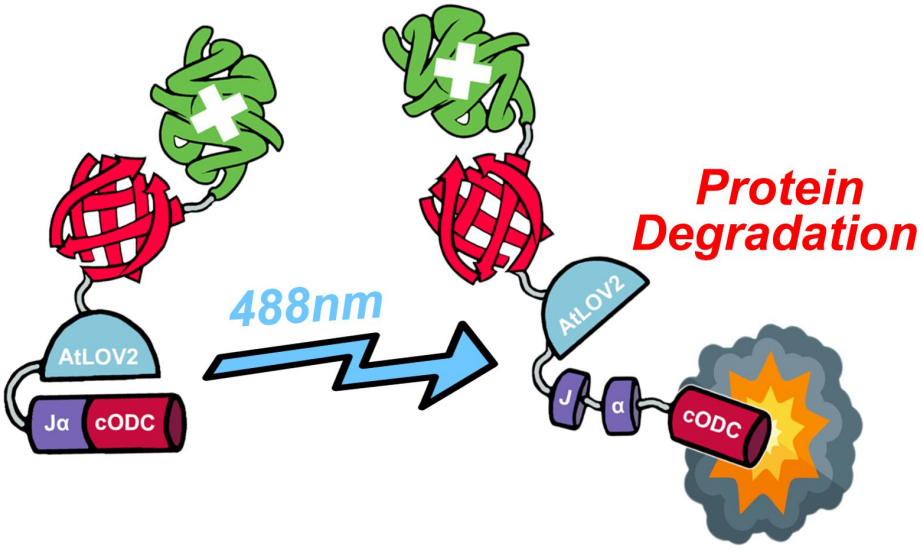
Protein Degradation
488nm
AtLOV2
Jα
cODC
AtLOV2
J
α
cODC

C

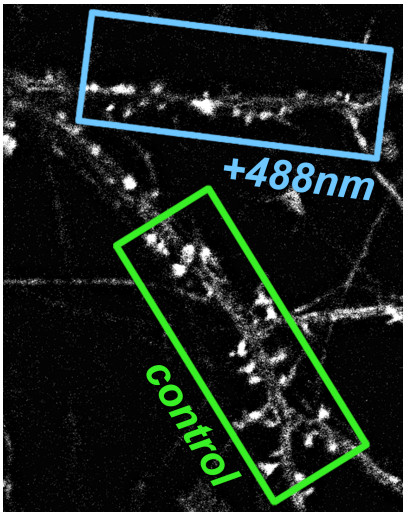
+488nm
control

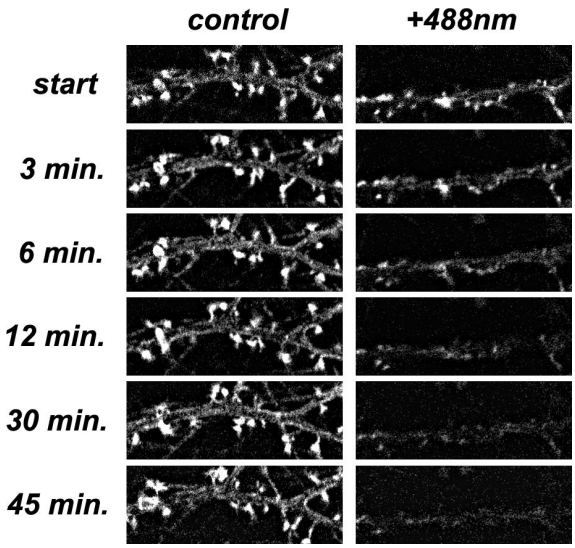
control
+488nm
start
3 min.
6 min.
12 min.
30 min.
45 min.

Fig. 6) Schematic and proof of principle experiment demonstrating optogenetic knockdown-rescue-degradation (KDRdeg).

(A) Diagram of DNA vector for knockdown-rescue-degradation (KDRdeg). **(B)** Diagram of rescue fusion protein, labeled with mScarlet, and a photo-sensitive degron (PSD), a chimeric AtLOV2 protein with its kinase domain replaced cODC proteasomal recognition sequence. Illumination with 488nm light results in a conformational change in the PSD, resulting in ubiquitination and destruction of the fusion protein. **(C)** Images of hippocampal dendrites from neurons transfected with KDRdeg and pulsed with 488nm laser light, showing loss of protein over time only in the illuminated section of dendrite.

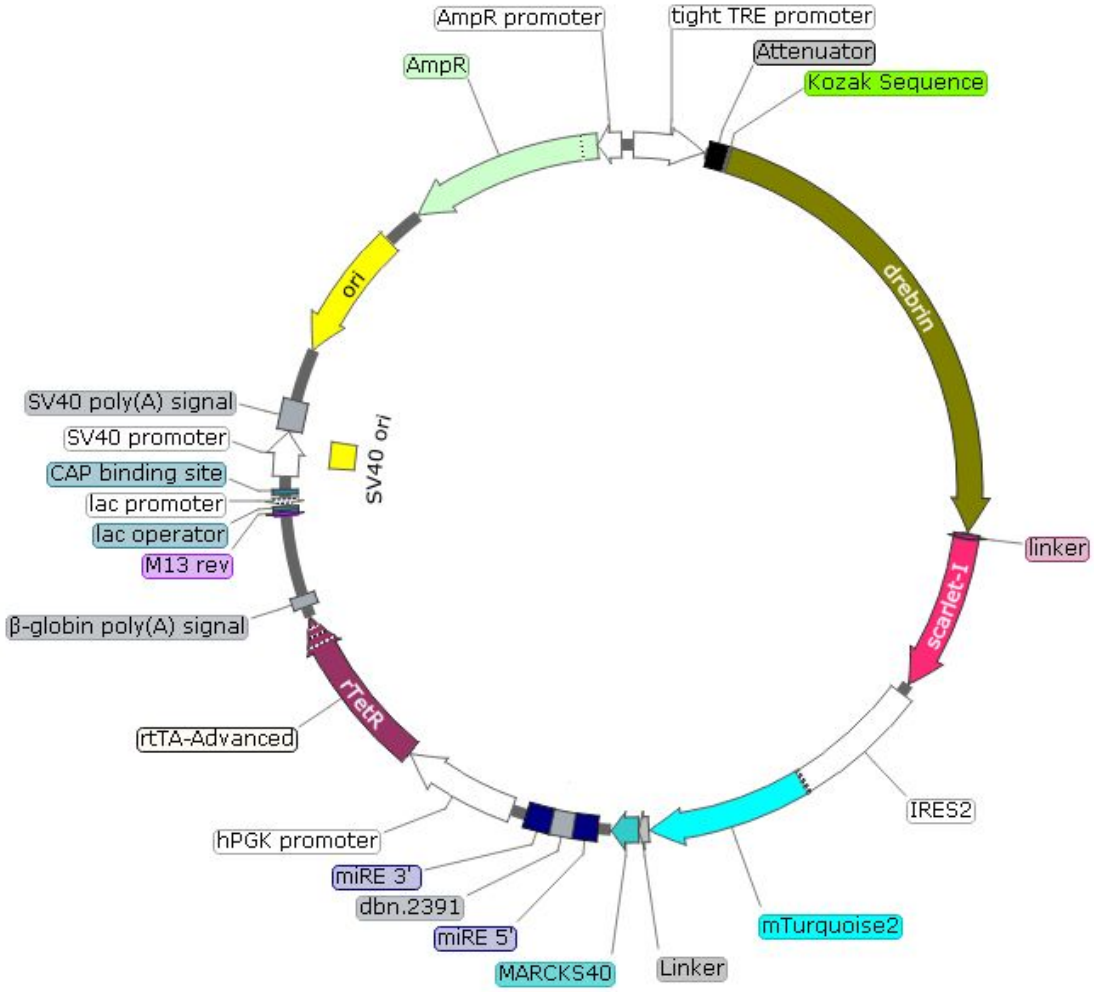

Supplemental Fig. 1) Complete pmAtt plasmid schematic.

Drebrin-RFP as example rescue gene, with corresponding endogenous drebrin 3' UTR-targeted miRNA, and pmTurquoise2 reporter variant is shown. As configured, the total plasmid size without rescue gene is only 7378 nucleotides.

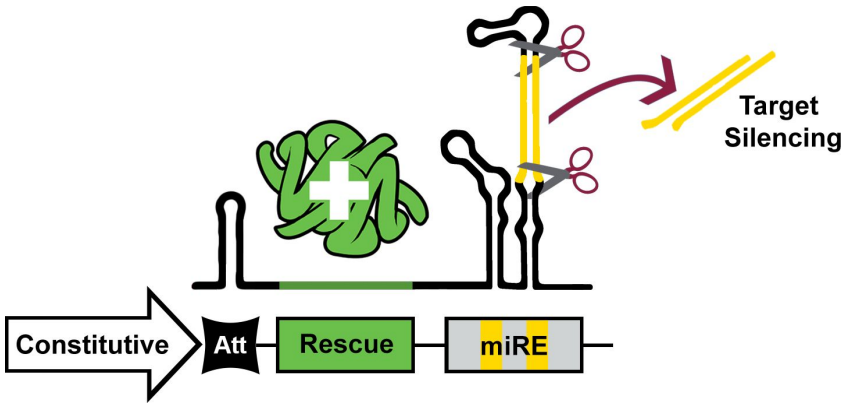

Supplemental Fig. 2) Minimal knockdown-rescue transcript.

Where viral packaging capacity is limited, or in applications where a fluorescent reported is unnecessary, this construct provides the greatest overhead for rescue gene size. This construct is designed to function with any promoter, and facilitate simple transfer to new vectors and delivery strategies as they mature.

Chapter 4

Conclusions and Future Directions

The human brain possesses an estimated 10 trillion dendritic spines (Nimchinsky et al., 2002) distributed among, conservatively, 100 billion neurons (Herculano-Houzel 2009). Plasticity of these tiny structures and synapses formed between other neurons requires changes in their individual molecular compositions (Hübener and Bonhoeffer, 2010). The primary goal of this dissertation has been to determine how changes in the actin cytoskeleton preferentially direct transient entry of microtubules (MTs), and thus cargo transported along them, to synaptically active dendritic spines. Our previous work indicated that both F-actin polymerization and drebrin expression are strongly positive regulators of invasions (Merriam et al., 2013). Based on these and other data our working model of spine invasion hypothesizes that activity-dependent changes in both actin and actin-associated proteins transiently regulate actin-MT interactions (Dent 2017). Given that drebrin and the MT plus end tracking protein EB3 had been implicated as direct binding partners (Geraldo et al., 2008), and this interaction may be enhanced by synaptic activity (Worth et al., 2013; McVicker et al., 2015), we sought to evaluate the relationship between these two proteins further.

In the first study (Chapter 2) we demonstrated that overexpression of EB3 promotes invasions, while EB1 overexpression diminishes them. Additionally, deleting residues in EB3 that were previously reported necessary for drebrin interaction, with the EB3Δi mutant knockdown-rescue (KDR), also diminishes MT invasions relative to wild type (WT) EB3. These results are consistent with previous observations that drebrin selectively binds EB3, but not EB1 (Geraldo et al., 2008), and with our own working model of spine invasion, where EB3 and drebrin might act as direct linkers to guide invasions. However, there are considerations to be made when interpreting these data. For one, fluorescently tagging EB proteins can affect their behavior. EB1 C-terminal tagging displaces CLIP-170, which links MT + ends and organelle membranes and is an anti-catastrophic factor (Skube et al., 2010). Despite this, most EB

constructs, including those used in the present study, employ C-terminal tags because N-terminal tagging is accepted to be more disruptive. EB1 N-terminal GFP fusion constructs significantly increase affinity for MTs and, likely by dimerization, act synergistically with endogenous EB1 proteins to influence their behavior as well (Zhu et al., 2009). To our knowledge it has not been documented whether EB3 mediates, or is subject to, similar effects. Fluorescent tubulin could be imaged in place of direct EB visualization to eliminate issues brought on by tagging, however, Skube et al., 2010 found that practically any manipulation of EB1 had varied, and largely unpredicted consequences. For example, expression of fragments of EB1 not expected to interact with CLIP-170 still displaced it, and additionally, while EB1 is typically protected from ubiquitin-dependent degradation by the COP9 signalosome (Peth et al., 2007), overexpression of fragments may reach saturation and lead to the degradation of endogenous protein (Skube et al., 2010). At present, the only notable alternative to these approaches for MT plus end visualization are natural SxIP motif-containing protein fragments (Honnappa et al., 2009) or artificial aptamers (Leśniewska et al., 2014). While these have been demonstrated to highlight actively polymerizing MTs, by nature they are effectively dominant negative constructs which risk displacement of +TIP complexes directly from their very foundation. Altogether, there is no “perfect” means of visualizing MT plus ends but so long as we remain cognizant of their individual caveats this does not devalue these experiments.

To build on experiments detailed in this dissertation we have generated several new chimeric EB constructs for future experiments. First, we need to further evaluate whether the residues deleted in the EB3Δi indeed function as an unconventional binding motif for drebrin, and to rule out the possibility that truncation has deleterious physical consequences unrelated to direct binding. Toward this goal, we swapped the region deleted in EB3Δi (AA 177-194) with the corresponding residues from EB1, and vice versa. We have termed these constructs EB131 and

EB313, where the middle numeral refers to the donor isoform. If indeed these minimally conserved residues impart special function to EB3 with respect to spine invasions we should expect to see those differences reflected by the increased rate of MT invasion with EB131 compared to EB1, and a decreased rate with EB313, compared to EB3. An alternative, or perhaps even additional, explanatory factor for these isoform differences is that +TIP complexes that have preference for one EB isoform over the other, differ in their ability to guide invasions. Such selectivity occurs naturally (Ferreira et al., 2013), and is conferred by the amino acids flanking both sides of the core SxIP sequence in +TIP proteins (Leśniewska et al., 2014). To test this possibility we generated complete C-terminal swap chimeras termed EB3c1, and EB1c3. If isoform-specific differences in +TIP complexes contribute in any way to invasions, based on data from the present study we expect that both chimeras would reflect their donor isoform. Additionally, others have mapped the residues of EB1 and EB3 necessary for SxIP-binding (Slep et al., 2005) contained within the C-terminal “APC-binding” domain of both proteins, named after its first identified binding partner (Su et al., 1995). Based on this, we created a SxIP-binding deficient EB3 mutant termed EB3ΔAPC to eliminate these interactions. Finally, since we expect EB1c3 to provide gain-of-function, we will also test an EB1c3ΔAPC construct, (chimeric EB1 with SxIP-binding deficient EB3 C-terminus) which should provide a highly informative comparison.

We observed a modest, but consistent and reproducible decrease in invasions with EB3Δi. To date, no EB3 binding motifs or regions are defined within drebrin. If proven to be direct, EB3 residues 177-194 represent a highly unconventional mode of interaction. Though our data do not prove this, it would of course not be unreasonable as researchers are continually discovering new EB-recognition motifs (Kumar et al., 2017). Amongst many other explanations, including additional intermediate partners, this left the possibility of alternate

modes of binding to drebrin. While SxIP motifs allow considerable sequence variability, core residues of both putative motifs present in drebrin had been described elsewhere (*SxLP in* Fong et al., 2009; *TxIP in* Geyer et al., 2015). However, there was ample rationale to investigate these motifs beyond amino acid sequence. Foremost, tandem SxIP motifs have been known to have greater affinity than lone motifs, possibly due to the natural dimerization of EB proteins (Honnappa et al., 2009; Buey et al., 2012). We showed that embryonic drebrin fails to promote invasions in the same manner as its adult isoform. In line with this, only one putative SxIP sequence is shared between both drebrin E and A, while a second is adjacent, within the adult-specific insert. As described earlier it is well established that SxIP motifs may exhibit isoform preference for EB1 or EB3 (Leśniewska et al., 2014). Though difficult to predict, this isoform preference could have entirely accounted for drebrin's preferential binding of EB3 instead of EB1. Despite this possibility, our drebrin A ΔSxIP construct had no impact on invasions, indicating that these two putative SxIP motifs in drebrin do not act as EB3 binding motifs with regard to MT invasions of spines.

Since beginning this project, a widening body of literature claims that direct drebrin-EB3 interaction is integral for a various cellular processes (Sonego et al., 2015; Ketschek et al., 2016; Dart et al., 2017; Trivedi et al., 2017; Zhao et al., 2017). However, only two groups have ever actually demonstrated immunoprecipitation (IP) of EB3 and drebrin, and did so in immortalized cell lines (Geraldo et al., 2008; Worth et al., 2013; Bazellières et al., 2012). Our own analysis of specific EB3-drebrin interaction has been made particularly challenging by our inability to replicate these results in primary neurons, even under modestly stringent conditions. For this same reason we must also be cautious in our interpretations. The results we present here do not conflict with our previous model of activity-dependent drebrin-EB3 interaction in

promoting MT invasions of spines. However, the distinct possibility that these are observations of synergistic, but ultimately independent, processes must be considered.

This failure to IP drebrin and EB3 together may also be reflective of the highly transient nature of this interaction. One attractive alternative to conventional IP is BioID, which employs proximity-based biotinylation to identify interactors (Kim et al., 2016). These covalent modifications should, in theory, permit us to capture transient interactions with much greater throughput than was previously possible. Other aspects of EB3-drebrin interaction will require further creative experimentation to probe. For example, we show that phosphomimetic drebrin S142D promotes invasions relative to a non-phosphorylatable S142A mutant. However, the same publication these experiments were based on reported this phosphorylation is not only permissive of EB3 binding, but that it also reveals cryptic actin bundling activity by drebrin. Given that we have shown F-actin polymerization is both necessary and sufficient for spine invasion (Merriam et al., 2013), the two possibilities become experimentally inextricable. Direct interaction notwithstanding, these experiments highlight specific and important contributions of both actin- and MT-associated proteins governing spine invasions, and thereby synaptic plasticity.

We also showed that actin-binding deficient drebrin (ΔABS) is incapable of promoting invasions in the manner of WT drebrin. This mutant appeared diffuse throughout neurons, in contrast to WT drebrin. In fact, drebrin ΔABS appears to act as a dominant-negative, presumably out-competing binding partners which would normally contribute to invasions. This strongly suggests that proper localization of drebrin to spines and ability to interact with F-actin is mandatory. This is complementary to our previous demonstrations that depleting drebrin with siRNA all but eliminates invasions (Merriam et al., 2013). An interesting complement to this experiment could employ the pharmacological agent 3,5-bis(trifluoromethyl)pyrazole (BTP),

which has shown promise as an anti-cancer drug, and is now understood to bind drebrin with specificity and dislodge it from F-actin (Mercer et al., 2010). Previous studies have shown that the residues responsible for drebrin's affinity for actin are extraordinarily widely distributed (Grintsevich et al., 2010), making it unrealistic to attempt to make point-mutations to eliminate drebrin-actin interactions. However, the BTP binding site on drebrin has been mapped to K270 and K271 in the human protein, and point mutations to these same residues (K270M, K271M) render it insensitive (Mercer et al., 2010). Interestingly, though Mercer et al. clearly illustrate that BTP prevents overexpressed drebrin from inducing aberrant filopodia formation, it does not appear to reduce overlapping staining with phalloidin. Considering this, BTP might provide a powerful means of teasing apart whether drebrin predominantly exerts effects on invasions via F-actin polymerization, if its localization and function as an actin-MT crosslinker is most important, or if other important contributions remain undiscovered. This could be further refined by employing our KDR strategy, wherein WT drebrin could be compared to BTN-insensitive (K270M, K271M) mutant as a control condition. We must also keep in mind that drebrin not only directly modifies actin, but also does so through complex competitive and cooperative action with other actin-associated proteins. We previously demonstrated that drebrin silencing with siRNA effectively eliminates invasions (Merriam et al., 2013). Irrespective of any other function, one explanation for this decrease in MT invasions of spines is massive dysregulation of the actin network. To name just a few, absence of drebrin should be expected to allow unchecked cleavage by cofilin (Grintsevich et al., 2014), aberrant f-actin bundling by fascin (Sasaki et al., 1996), and cross-linking by α-actinin (Ishikawa et al., 1994). When depleted, the complex interplay between all these proteins responsible for actin dynamics could be thrown out of balance severely enough to explain, on its own, the deficits seen with invasion rates.

An elephant in the room, though remarkably common in knockout animals (El-Brolosy, et al., 2017), is that there is positively nothing wrong with homozygous drebrin knockout mice (Willmes et al., 2017). Analysis of gross brain and neuronal morphology revealed no phenotype resulting from its absence. Electrophysiological recordings in acute hippocampal slices and primary hippocampal neuronal cultures showed that basal synaptic transmission, and both long-term and homeostatic synaptic plasticity were unchanged. This is in stark contrast to the drebrin A-selective knockout mouse (*DAKO,* Kojima et al., 2010 & 2016) which, while largely intact ultrastructurally, exhibits deficits in hippocampal LTP and hippocampus-dependent fear conditioning. Likely, robust compensatory mechanisms exist and may themselves be illuminating. Our own results indicate that some unique function of drebrin's adult-specific insert facilitates MT invasions of spines and have ruled out direct, SxIP-facilitated association as we originally suspected might be explanatory. Certainly, additional careful analysis must be done to completely understand the functions of this protein.

As a final note, compared to the present study, it is apparent that initial characterizations of spine invasions in our laboratory dramatically under-reported their frequency (Hu et al., 2008; Merriam et al., 2011; Merriam et al., 2013). These previous studies documented ~10% of spines were invaded by a polymerizing MT in an hour of imaging, while the present studies (Ch. 2, Fig. 5) show the percentage of spines invaded as ~20% in 10 minutes of imaging. The likeliest explanation for this is that total internal reflection fluorescence (TIRF) microscopy was used almost exclusively to achieve sufficient signal-to-noise for visualizing the behavior of individual MTs in all our previously published studies. The primary advantage of TIRF microscopy is that it delivers exceptional images within an extremely thin ~200nm optical slice (Fish 2009). The caveat to this technique is that the optical slice is only the ~200nm immediately above the coverslip. Because of this imaging limitation, low-density neuronal cultures supported by

media-conditioning, glia-coated “feeder” cover slips oriented above, but not touching, the neuronal layer on the coverslip, were necessary for maintaining long-term hippocampal cultures, while being able to image dendritic spines positioned directly on the coverslip. With a newly acquired confocal microscope we have been able to culture neurons at higher density ($3x10^4/cm^2$ compared to $5x10^3/cm^2$ for TIRF studies). While we have invested great effort refining our expression plasmids to improve our ability to visualize EB comets, we suspect this marked increase in invasion rates is explained primarily by increased quality of cultures. A greater density of neurons overall should translate to more functional connections, and greater global activity. Additionally, low density cultures require proliferative inhibitors (cytosine arabinoside (ara-C)) to prevent glia from over-proliferating and dominating cover-slips (Viesselmann et al., 2011). We do not observe this overgrowth in high-density neuronal cultures and, given the increasingly-appreciated supportive role glia play in nervous system development, synaptogenesis, plasticity (Min et al., 2012; Schafer et al., 2015; Tadi et al., 2015), it is tempting to speculate that this represents an environment more akin to whole organisms than we previously achieved.

In the second study (Chapter 3) we devised and constructed a novel plasmid-based system for inducible and reversible replacement of target genes. This was initially conceived as a way to overcome technical hurdles encountered while evaluating the effects of targeted mutations in mature neurons. Specifically, we tried to minimize the obfuscating contributions of endogenous protein in dominant-negative studies, while preserving earlier developmental stages, where proteins may be functioning in similar or different processes as they do in mature neurons. Having surmounted these issues, we demonstrated on-cue turnover of drebrin in mature hippocampal neurons with drebrin-GFP, and later refined this technique to allow physiological tuning on a protein-to-protein basis. We achieved this by combining a tet-inducible

promoter and transactivator, which are heavily engineered staples of modern expression systems, with natural regulatory elements of mammalian untranslated regions (UTR), which are vastly overlooked in such applications. Future development of this technique may incorporate an ever-increasing wealth of information pertaining to UTR elements in their control of translation to further tune and refine the function of this platform. Of particular interest are elements which permit rapid inhibition of translation of existing mRNA transcripts in responsive to a diverse range of cellular conditions, including but not limited to metabolic cues (Leppek et al., 2018). To expand on the present study, we plan to create a small library of varying intensity attenuator sequences. We expect that the accessibility of this technique would be increased by facilitating the matching of endogenous expression of the protein of interest to its expression downstream of a pre-defined range of translation-limiting hairpins.

To date, we have used this knockdown-replacement (KDR) platform as a means of perturbing healthy cells to understand the effects of targeted mutations. In Chapter 2 (Fig. 5) we employed this technique to introduce either wild type (WT) controls or experimental constructs in place of endogenous counterparts. However, in the case of diseases with genetic etiology, we envision the reverse is also quite possible, where this technique could be instead applied as a genetically engineered strategy to replace mutant with functional proteins. We are currently preparing to do precisely this in models of human leukodystrophy and amyotrophic lateral sclerosis, two crippling and poorly understood diseases with no current cure. These studies, funded through the European Leukodystrophy Association and the University of Wisconsin Institute for Clinical and Translational Research, respectively, will be valuable demonstrations of efficacy. Importantly, despite recent notable successes, including treatment of the fatal neurodegenerative condition adrenoleukodystrophy (ALD) (Eichler et al., 2017), genetic therapy remains one of the greatest challenges in modern medicine. Features intrinsic to

neurodegenerative disorders compound this difficulty in treatment. Many diseases may be treatable with patient-derived cells that are cultured in the laboratory, genetically modified via CRISPR/Cas9 technology, screened extensively and then re-introduced. However, this process of treatment is not possible with most diseases of the central nervous system because the vast majority of neurons are terminally postmitotic and, with regard to memory, engaged in networks which must be preserved. As such, successful treatment would require systemic administration of therapeutics. Because of this natural immunity to viral vectors becomes a major barrier to genetic manipulation and makes second attempts rare (Colella et al., 2018). As we slowly but inexorably move toward personalized medicine, pre-validation of treatments in patient derived cells will one day become a reality. Therefore, though tools used in primary research are seldom directly translatable to clinical application, we should strive to design materials with this lofty but altogether possible application in mind. Our vector-agnostic, single transcript design brings unique advantages suited to this. Foremost, strategies proven effective *in vitro* could be transferred directly to any appropriate, approved vector, and is compatible with chromosomal insertion by retroviral integration or other means, or episomal persistence (Colella et al., 2018). This also means future advances in viral therapeutics may be harnessed without undue complication, enhancing, rather than antiquating, this strategy. Additionally, with systemic administration therapy must often be targeted to a specific cell type, and most, if not all affected cells to be effective. rAAV serotypes can help with this, and as this technique is compatible with essentially any promoter, cell type-specific variants of both could be employed in complementary manner. It is worth noting that rAAV viral packaging limits space to a precious commodity (Wu et al., 2010). Our strategy aids in this as well, as both rescue gene and miRNA from a single transcript, allowing larger genes to be included in the construct. Altogether, it is our hope that the toolkit we described in this work proves widely useful not only for

understanding conditions which adversely impact human health, but also in the direct application of materials to combat them.

References

Bazellières E, Massey-harroche D, Barthélémy-requin M, Richard F, Arsanto JP, Le bivic A. Apico-basal elongation requires a drebrin-E-EB3 complex in columnar human epithelial cells. J Cell Sci. 2012;125(Pt 4):919-31.

Buey RM, Mohan R, Leslie K, et al. Insights into EB1 structure and the role of its C-terminal domain for discriminating microtubule tips from the lattice. Mol Biol Cell. 2011;22(16):2912-23.

Colella P, Ronzitti G, Mingozzi F. Emerging Issues in AAV-Mediated Gene Therapy. Mol Ther Methods Clin Dev. 2018;8:87-104.

Dart AE, Worth DC, Muir G, et al. The drebrin/EB3 pathway drives invasive activity in prostate cancer. Oncogene. 2017;36(29):4111-4123.

Dent EW. Of microtubules and memory: implications for microtubule dynamics in dendrites and spines. Mol Biol Cell. 2017;28(1):1-8.

Eichler F, Duncan C, Musolino PL, et al. Hematopoietic Stem-Cell Gene Therapy for Cerebral Adrenoleukodystrophy. N Engl J Med. 2017;377(17):1630-1638.

El-Brolosy MA, Stainier DYR. Genetic compensation: A phenomenon in search of mechanisms. PLoS genetics. 2017; 13(7):e1006780.

Ferreira JG, Pereira AJ, Akhmanova A, Maiato H. Aurora B spatially regulates EB3 phosphorylation to coordinate daughter cell adhesion with cytokinesis. J Cell Biol. 2013;201(5):709-24.

Geraldo S, Khanzada UK, Parsons M, Chilton JK, Gordon-weeks PR. Targeting of the F-actin-binding protein drebrin by the microtubule plus-tip protein EB3 is required for neuritogenesis. Nat Cell Biol. 2008;10(10):1181-9.

Grintsevich EE, Reisler E. Drebrin inhibits cofilin-induced severing of F-actin. Cytoskeleton (Hoboken). 2014;71(8):472-83.

Herculano-Houzel S. The human brain in numbers: a linearly scaled-up primate brain. Front Hum Neurosci. 2009;3:31.

Honnappa S, Gouveia SM, Weisbrich A, et al. An EB1-binding motif acts as a microtubule tip localization signal. Cell. 2009;138(2):366-76.

Hu X, Viesselmann C, Nam S, Merriam E, Dent EW. Activity-dependent dynamic microtubule invasion of dendritic spines. J Neurosci. 2008;28(49):13094-105.

Hübener M, Bonhoeffer T. Searching for engrams. Neuron. 2010;67(3):363-71.

Ishikawa R, Hayashi K, Shirao T, et al. Drebrin, a development-associated brain protein from rat embryo, causes the dissociation of tropomyosin from actin filaments. J Biol Chem. 1994;269(47):29928-33.

Ketschek A, Spillane M, Dun XP, Hardy H, Chilton J, Gallo G. Drebrin coordinates the actin and microtubule cytoskeleton during the initiation of axon collateral branches. Dev Neurobiol. 2016;76(10):1092-110.

Kim DI, Jensen SC, Noble KA, et al. An improved smaller biotin ligase for BioID proximity labeling. Mol Biol Cell. 2016;27(8):1188-96.

Kumar A, Manatschal C, Rai A, et al. Short Linear Sequence Motif LxxPTPh Targets Diverse Proteins to Growing Microtubule Ends. Structure. 2017;25(6):924-932.e4.

Leppek K, Das R, Barna M. Functional 5' UTR mRNA structures in eukaryotic translation regulation and how to find them. Nat Rev Mol Cell Biol. 2018;19(3):158-174.

Leśniewska K, Warbrick E, Ohkura H. Peptide aptamers define distinct EB1- and EB3-binding motifs and interfere with microtubule dynamics. Mol Biol Cell. 2014;25(7):1025-36.

McVicker DP, Millette MM, Dent EW. Signaling to the microtubule cytoskeleton: an unconventional role for CaMKII. Dev Neurobiol. 2015;75(4):423-34.

Mercer JC, Qi Q, Mottram LF, et al. Chemico-genetic identification of drebrin as a regulator of calcium responses. Int J Biochem Cell Biol. 2010;42(2):337-45.

Merriam EB, Lumbard DC, Viesselmann C, et al. Dynamic microtubules promote synaptic NMDA receptor-dependent spine enlargement. PLoS ONE. 2011;6(11):e27688.

Merriam EB, Millette M, Lumbard DC, et al. Synaptic regulation of microtubule dynamics in dendritic spines by calcium, F-actin, and drebrin. J Neurosci. 2013;33(42):16471-82.

Min R, Nevian T. Astrocyte signaling controls spike timing-dependent depression at neocortical synapses. Nat Neurosci. 2012;15(5):746-53.

Nimchinsky EA, Sabatini BL, Svoboda K. Structure and function of dendritic spines. Annu Rev Physiol. 2002;64:313-53.

Peth A, Boettcher JP, Dubiel W. Ubiquitin-dependent proteolysis of the microtubule end-binding protein 1, EB1, is controlled by the COP9 signalosome: possible consequences for microtubule filament stability. J Mol Biol. 2007;368(2):550-63.

Sasaki Y, Hayashi K, Shirao T, Ishikawa R, Kohama K. Inhibition by drebrin of the actin-bundling activity of brain fascin, a protein localized in filopodia of growth cones. J Neurochem. 1996;66(3):980-8.

Schafer DP, Stevens B. Microglia Function in Central Nervous System Development and Plasticity. Cold Spring Harb Perspect Biol. 2015;7(10):a020545.

Skube SB, Chaverri JM, Goodson HV. Effect of GFP tags on the localization of EB1 and EB1 fragments in vivo. Cytoskeleton (Hoboken). 2010;67(1):1-12.

Slep KC, Rogers SL, Elliott SL, Ohkura H, Kolodziej PA, Vale RD. Structural determinants for EB1-mediated recruitment of APC and spectraplakins to the microtubule plus end. J Cell Biol. 2005;168(4):587-98.

Sonego M, Oberoi M, Stoddart J, et al. Drebrin regulates neuroblast migration in the postnatal mammalian brain. PLoS ONE. 2015;10(5):e0126478.

Su LK, Burrell M, Hill DE, et al. APC binds to the novel protein EB1. Cancer Res. 1995;55(14):2972-7.

Tadi M, Allaman I, Lengacher S, Grenningloh G, Magistretti PJ. Learning-Induced Gene Expression in the Hippocampus Reveals a Role of Neuron -Astrocyte Metabolic Coupling in Long Term Memory. PLoS ONE. 2015;10(10):e0141568.

Trivedi N, Stabley DR, Cain B, et al. Drebrin-mediated microtubule-actomyosin coupling steers cerebellar granule neuron nucleokinesis and migration pathway selection. Nat Commun. 2017;8:14484.

Willmes CG, Mack TG, Ledderose J, Schmitz D, Wozny C, Eickholt BJ. Investigation of hippocampal synaptic transmission and plasticity in mice deficient in the actin-binding protein Drebrin. Sci Rep. 2017;7:42652.

Worth DC, Daly CN, Geraldo S, Oozeer F, Gordon-weeks PR. Drebrin contains a cryptic F-actin-bundling activity regulated by Cdk5 phosphorylation. J Cell Biol. 2013;202(5):793-806.

Wu Z, Yang H, Colosi P. Effect of genome size on AAV vector packaging. Mol Ther. 2010;18(1):80-6.

Zhao B, Meka DP, Scharrenberg R, et al. Microtubules Modulate F-actin Dynamics during

Neuronal Polarization. Sci Rep. 2017;7(1):9583.

Zhu ZC, Gupta KK, Slabbekoorn AR, Paulson BA, Folker ES, Goodson HV. Interactions between EB1 and microtubules: dramatic effect of affinity tags and evidence for cooperative behavior. J Biol Chem. 2009;284(47):32651-61.